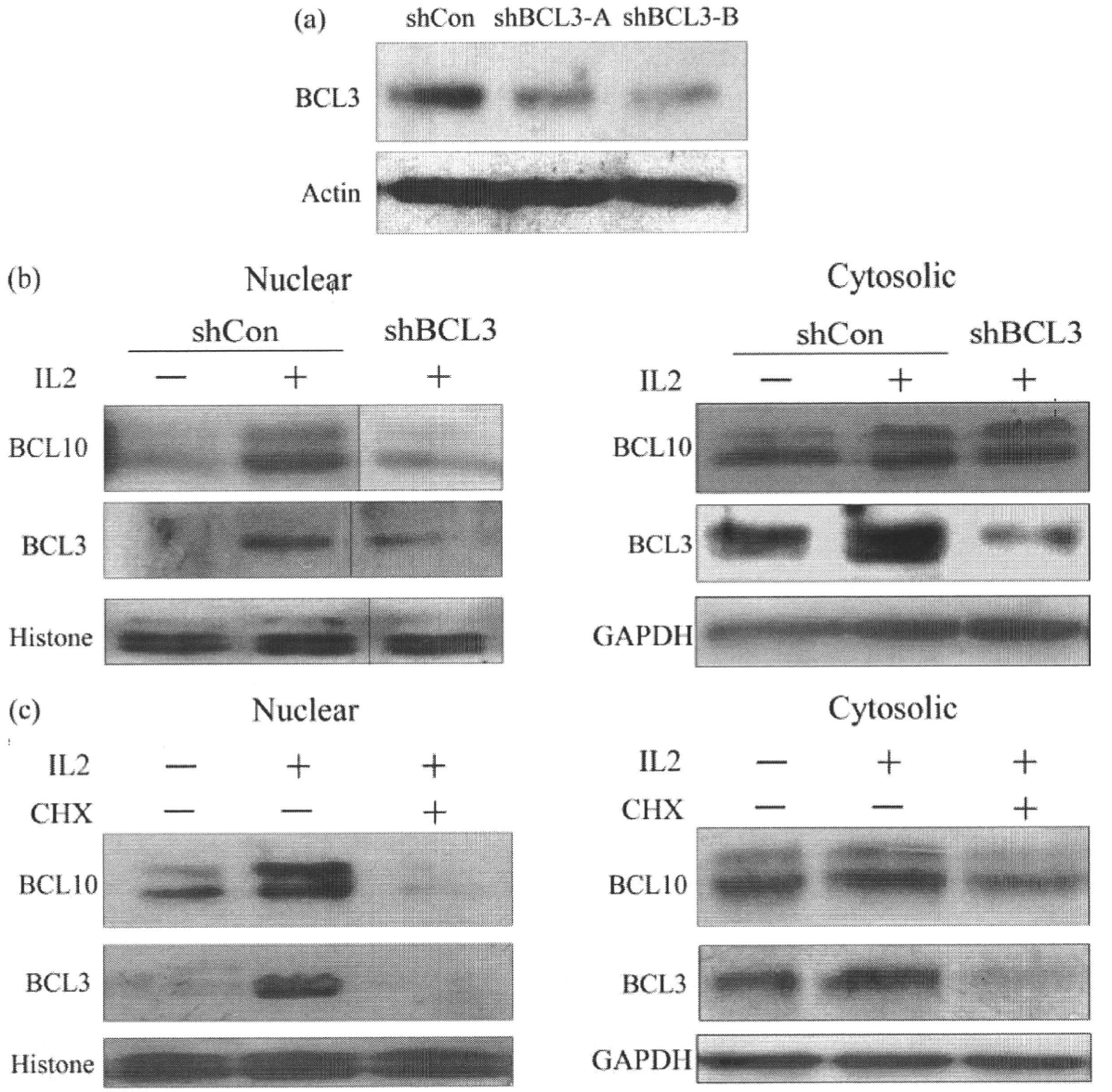

Figure 8. Knockdown of BCL3 expression by shRNA or CHX affects the nuclear localization of BCL10. (a) Immunoblotting results for BCL3 in SNK-6 cells. The expression of BCL3 was knocked down using two shRNA sequences. Actin served as the normalization control for immunoblotting. (b) Immunoblotting result for BCL10 and BCL3 in the nuclear and cytosolic extracts. shRNA-transduced SNK-6 cells were grown in the presence or absence of IL2 (300 U/ml) before cellular fractionation. (c) Immunoblotting results for BCL10 and BCL3 in the nuclear and cytosolic extracts. NK-YS cells were treated with IL2 in the presence or absence of 80 μg/ml CHX for 24 h before cellular fractionation. For b and c, GAPDH and histone were used as loading controls for the cytosolic and nuclear extracts, respectively.

[44,45]. Here we have provided evidence that BCL10 also participates in cytokine receptor-induced NF-κB signalling. Similar to the role of PKC in antigen receptor signalling, Akt is the kinase responsible for signal transduction via the IL2 receptor. Downstream of these kinases, BCL10 acts as a conductor to orchestrate NF-κB activation signalling, which is linked to different receptors, suggesting that BCL10 is a crucial adaptor in immune cells.

The nuclear localization of BCL10 is a recurrent phenomenon associated with MALT lymphoma and ENKL [4,46], indicating that aberrant nuclear BCL10 expression might play a role in the development of these diseases. Moreover, a distinct group of MALT lymphoma patients have shorter failure-free survival associated with the presence of nuclear BCL10 [47]. Thus, the identification of mechanisms that regulate the subcellular localization of BCL10 may be beneficial. An earlier report indicated that BCL3, a member of the IκB family, may be a binding partner of BCL10 in the nucleus [25]. That study focused on the human breast carcinoma cell line MCF7, however, raising concerns that the findings may not be representative of the actions of BCL3 in lymphoid cells. Kuo *et al* recently reported that B-cell activating factor (BAFF), a tumour necrosis factor-related cytokine, induces the nuclear transfer of BCL10 via BCL3 in the B-cell lymphoma cell line Pfeiffer [30]. Here we have described a similar

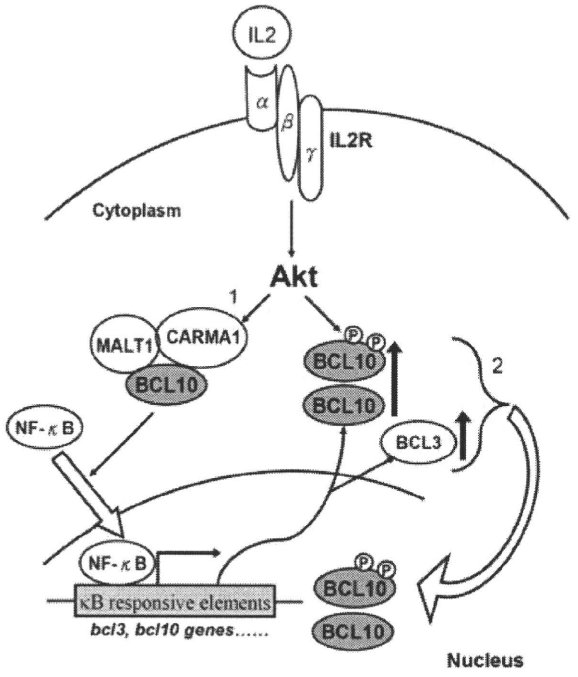

Figure 9. Schematic diagram of BCL3/BCL10-mediated NF-κB signalling modulation in ENKL. (1) Engagement of the IL2 receptor with IL2 activates the canonical NF-κB signalling pathway via Akt and this leads to a global increase in the expression of NF-κB-responsive genes. BCL3 and BCL10 expression are up-regulated and more protein appears in the cytosol. A circuit of BCL10 overexpression forms and promotes NF-κB activation. (2) On the other hand, BCL3 binds to BCL10 and facilitates BCL10 nuclear translocation. The level of BCL10 decreases in the cytosol and formation of the CARMA1–BCL10–MALT1 signalosome is inhibited. This negative feedback modulates NF-κB signalling.

scenario, demonstrating that IL2 induces the nuclear localization of both BCL3 and BCL10 in ENKL cells. This study provides an underlying mechanism for the nuclear translocation of BCL10 and more significantly, we have identified the essential role of BCL10 that connects IL2 receptor signalling with NF-κB activation. Because IL2 is a cytokine that plays a crucial role in the proliferation and development of T, B, and NK cells [48], the identification of BCL10 in the NK-cell activation signalling pathway that links the IL2 receptor with NF-κB activation is of great significance.

In Figure 8 we show that BCL10 nuclear translocation is dependent on the availability of BCL3. When BCL3 was silenced by RNA interference, BCL10 nuclear translocation was suppressed accordingly. Furthermore, when overall protein translation was suppressed by CHX, the nuclear transfer of BCL10 was diminished. This indicates that the nuclear translocation of BCL3 and BCL10 is dependent on the availability of new proteins, which are continuously generated. Overexpression of BCL3 may promote the nuclear translocation of BCL10. On the other hand, BCL3 is a member of the IκB family that does not act on the IKK complex. It plays a role as an NF-κB co-activator in the nucleus and is believed to be oncogenic [49]. Overexpression of BCL3 has been detected in multiple types of leukaemias and lymphomas [50]. Besides its role as a BCL10 binding partner, BCL3 has other roles that may also contribute to tumourigenesis.

As shown in Figure 9, up-regulation of BCL10 expression may occur via NF-κB binding to its potential 5′ UTR [25], which will transduce more activating signals through the amplification loop from BCL10 to NF-κB. The excess amount of BCL10 may exceed the number of MALT1 molecules, allowing BCL10 to escape cytosolic retention by MALT1 and enter into the nucleus [8,51]. Up-regulation of BCL3 would allow it to carry more BCL10 into the nucleus. If more BCL10 translocates into nucleus, the excess of BCL10 in the cytosol—where the CARMA1–BCL10–MALT1 signalosome is formed and plays a role in NF-κB signalling—would be reduced. Therefore, nuclear translocation of BCL10 is a result of NF-κB activation and in turn, it is used to modulate NF-κB signalling. A recent report also suggested that BCL10 in the nucleus is subject to degradation via the proteasome [52]. Thus, the nuclear translocation of BCL10 could represent a feedback mechanism that modulates 'exaggerated' NF-κB signalling. Other functions of nuclear BCL10, however, remain to be determined.

In summary, we have identified a critical role for BCL10 in cytokine receptor-induced NF-κB signalling, which results in NK cell activation. We also determined the underlying mechanism of the nuclear translocation of BCL10, which was found to be associated with constitutive NF-κB activation. Given that knockdown of BCL10 by shBCL10 suppressed the IL2-induced entry of SNK-6 cells into the G2/M phase of the cell cycle (an anti-proliferative effect), silencing of BCL10 might be a potential therapeutic option to kill ENKL tumour cells.

Acknowledgment

This study was supported by the General Research Fund (GRF) of the Research Grants Council of Hong Kong, China (HKU 7583/54M to GS and RHS).

References

1. Jaffe E, Chan J, Su I, Frizzera G, Mori S, Feller AC, *et al.* Report of the workshop on nasal and related extranodal angiocentric T/natural killer cell lymphomas. Definitions, differential diagnosis, and epidemiology. *Am J Surg Pathol* 1996; **20**: 103–111.
2. Chiang A, Chan A, Srivastava G, Ho F. Nasal NK/T-cell lymphomas are derived from Epstein–Barr virus-infected cytotoxic lymphocytes of both NK- and T-cell lineage. *Int J Cancer* 1997; **73**: 332–338.
3. Kaneko T, Fukuda J, Yoshihara T, Zheng H, Mori S, Mizoguchi H, *et al.* Nasal natural killer (NK) cell lymphoma: report of a case with activated NK cells containing Epstein–Barr virus and expressing CD21 antigen, and comparative studies of their phenotype and cytotoxicity with normal NK cells. *Br J Haematol* 1995; **91**: 355–361.
4. Shen L, Liang ACT, Lu L, Au WY, Wong KY, Tin PC, *et al.* Aberrant BCL10 nuclear expression in nasal NK/T-cell lymphoma. *Blood* 2003; **102**: 1553–1554.

5. Willis TG, Jadayel DM, Du MQ, Peng H, Perry AR, Abdul-Rauf M, *et al.* Bcl10 is involved in t(1;14)(p22;q32) of MALT B cell lymphoma and mutated in multiple tumor types. *Cell* 1999; **96**: 35–45.
6. Ye H, Dogan A, Karran L, Willis TG, Chen L, Wlodarska I, *et al.* BCL10 expression in normal and neoplastic lymphoid tissue. *Am J Pathol* 2000; **157**: 1147–1154.
7. Hu S, Du MQ, Park SM, Alcivar A, Qu L, Gupta S, *et al.* cIAP2 is a ubiquitin protein ligase for BCL10 and is dysregulated in mucosa-associated lymphoid tissue lymphomas. *J Clin Invest* 2006; **116**: 174–181.
8. Nakagawa M, Hosokawa Y, Yonezumi M, Izumiyama K, Suzuki R, Tsuzuki S, *et al.* MALT1 contains nuclear export signals and regulates cytoplasmic localization of BCL10. *Blood* 2005; **106**: 4210–4216.
9. Thome M. CARMA1, BCL10 and MALT1 in lymphocyte development and activation. *Nature Rev Immunol* 2004; **4**: 348–359.
10. Lucas PC, McAllister-Lucas LM, Nunez G. NF-κB signaling in lymphocytes: a new cast of characters. *J Cell Sci* 2004; **117**: 31–39.
11. Ruland J, Duncan GS, Elia A, Barrantes IB, Nguyen L, Plyte S, *et al.* Bcl10 is a positive regulator of antigen receptor-induced activation of NF-κB and neural tube closure. *Cell* 2001; **104**: 33–42.
12. Wegener E, Krappmann D. CARD–Bcl10–Malt1 signalosomes: missing link to NF-κB. *Sci STKE* 2007; **384**: pe21.
13. Malarkannan S, Regunathan J, Chu H, Kutlesa S, Chen Y, Zeng H, *et al.* Bcl10 plays a divergent role in NK cell-mediated cytotoxicity and cytokine generation. *J Immunol* 2007; **179**: 3752–3762.
14. Gross O, Grupp C, Steinberg C, Zimmermann S, Strasser D, Hannesschläger N, *et al.* Multiple ITAM-coupled NK-cell receptors engage the Bcl10/Malt1 complex via Carma1 for NF-κB and MAPK activation to selectively control cytokine production. *Blood* 2008; **112**: 2421–2428.
15. Cozen W, Gill P, Salam M, Nieters A, Masood R, Cockburn M, *et al.* Interleukin-2, interleukin-12, and interferon-gamma levels and risk of young adult Hodgkin lymphoma. *Blood* 2008; **111**: 3377–3382.
16. Chopra CG, Chitalkar LCP, Jaiprakash MGM. Cytokines: as useful prognostic markers in lymphoma cases. *Med J Armed Forces India* 2004; **60**: 45–49.
17. Su H, Orange J, Fast L, Chan A, Simpson S, Terhorst C, *et al.* IL-2-dependent NK cell responses discovered in virus-infected β_2-microglobulin-deficient mice. *J Immunol* 1994; **153**: 5674–5681.
18. Zhang Y, Nagata H, Ikeuchi T, Mukai H, Oyoshi MK, Demachi A, *et al.* Common cytological and cytogenetic features of Epstein–Barr virus (EBV)-positive natural killer (NK) cells and cell lines derived from patients with nasal T/NK-cell lymphomas, chronic active EBV infection and hydroa vacciniforme-like eruptions. *Br J Haematol* 2003; **121**: 805–814.
19. Fehniger T, Cooper M, Nuovo G, Cella M, Facchetti F, Colonna M, *et al.* $CD56^{bright}$ natural killer cells are present in human lymph nodes and are activated by T cell-derived IL-2: a potential new link between adaptive and innate immunity. *Blood* 2003; **101**: 3052–3057.
20. Zhou J, Zhang J, Lichtenheld MG, Meadows GG. A role for NF-κB activation in perforin expression of NK cells upon IL-2 receptor signaling. *J Immunol* 2002; **169**: 1319–1325.
21. Burchilla MA, Yanga J, Vanga KB, Farrar MA. Interleukin-2 receptor signaling in regulatory T cell development and homeostasis. *Immunol Lett* 2007; **114**: 1–8.
22. Jiang K, Zhong B, Ritchey C, Gilvary DL, Hong-Geller E, Wei S, *et al.* Regulation of Akt-dependent cell survival by Syk and Rac. *Blood* 2003; **101**: 236–244.
23. Narayan P, Holt B, Tosti R, Kane LP. CARMA1 is required for Akt-mediated NF-κB activation in T cells. *Mol Cell Biol* 2006; **26**: 2327–2336.
24. Kane LP, Shapiro VS, Stokoe D, Weiss A. Induction of NF-κB by the Akt/PKB kinase. *Curr Biol* 1999; **9**: 601–604.
25. Yeh PY, Kuo SH, Yeh KH, Chuang SE, Hsu CH, Chang WC, *et al.* A pathway for tumor necrosis factor-α-induced BCL10 nuclear translocation. BCL10 is up-regulated by NF-κB and phosphorylated by Akt1 and then complexes with BCL3 to enter the nucleus. *J Biol Chem* 2006; **281**: 167–175.
26. Matsuo Y, Drexler HG. Immunoprofiling of cell lines derived from natural killer-cell and natural killer-like T-cell leukemia–lymphoma. *Leuk Res* 2003; **27**: 935–945.
27. Hu Y, Qiao L, Wang S, Rong SB, Meuillet EJ, Berggren M, *et al.* 3-(Hydroxymethyl)-bearing phosphatidylinositol ether lipid analogues and carbonate surrogates block PI3-K, Akt, and cancer cell growth. *J Med Chem* 2000; **43**: 3045–3051.
28. Huang C, Bi E, Hu Y, Deng W, Tian Z, Dong C, *et al.* A novel NF-κB binding site controls human granzyme B gene transcription. *J Immunol* 2006; **176**: 4173–4181.
29. Yemelyanov A, Gasparian A, Lindholm P, Dang L, Pierce JW, Kisseljov F, *et al.* Effects of IKK inhibitor PS1145 on NF-κB function, proliferation, apoptosis and invasion activity in prostate carcinoma cells. *Oncogene* 2006; **25**: 387–398.
30. Kuo SH, Yeh PY, Chen LT, Wu MS, Lin CW, Yeh KH, *et al.* Overexpression of B cell-activating factor of TNF family (BAFF) is associated with *Helicobacter pylori*-independent growth of gastric diffuse large B-cell lymphoma with histologic evidence of MALT lymphoma. *Blood* 2008; **112**: 2927–2934.
31. Nacinović-Duletić A, Stifter S, Dvornik S, Skunca Z, Jonjić N. Correlation of serum IL-6, IL-8 and IL-10 levels with clinicopathological features and prognosis in patients with diffuse large B-cell lymphoma. *Int J Lab Haematol* 2008; **30**: 230–239.
32. Skinnider BF, Mak TW. The role of cytokines in classical Hodgkin lymphoma. *Blood* 2002; **99**: 4283–4297.
33. Dong G, Liu C, Ye H, Gong L, Zheng J, Li M, *et al.* BCL10 nuclear expression and t(11;18)(q21;q21) indicate nonresponsiveness to *Helicobacter pylori* eradication of Chinese primary gastric MALT lymphoma. *Int J Hematol* 2008; **88**: 516–523.
34. Yeh KH, Kuo SH, Chen LT, Mao TL, Doong SL, Wu MS, *et al.* Nuclear expression of BCL10 or nuclear factor-κB helps predict *Helicobacter pylori*-independent status of low-grade gastric mucosa-associated lymphoid tissue lymphomas with or without t(11;18)(q21;q21). *Blood* 2005; **106**: 1037–1041.
35. Isobe Y, Sugimoto K, Yang L, Tamayose K, Egashira M, Kaneko T, *et al.* Epstein–Barr virus infection of human natural killer cell lines and peripheral blood natural killer cells. *Cancer Res* 2004; **64**: 2167–2174.
36. Lambert S, Martinez O. Latent membrane protein 1 of EBV activates phosphatidylinositol 3-kinase to induce production of IL-10. *J Immunol* 2007; **179**: 8225–8234.
37. Najjar I, Baran-Marszak F, Clorennec CL, Laguillier C, Schischmanoff O, Youlyouz-Marfak I, *et al.* Latent membrane protein 1 regulates STAT1 through NF-κB-dependent interferon secretion in Epstein–Barr virus-immortalized B cells. *J Virol* 2005; **79**: 4936–4943.
38. Ho JW, Liang RH, Srivastava G. Differential cytokine expression in EBV positive peripheral T cell lymphomas. *Mol Pathol* 1999; **52**: 269–274.
39. Tao Q, Chiang AK, Srivastava G, Ho FC. TCR-CD56+CD2+ nasal lymphomas with membrane-localized CD3 positivity: are the CD3+ cells neoplastic or reactive? *Blood* 1995; **85**: 2993–2996.
40. Shen L, Liang AK, Liu WP, Li PD, Liang RH, Srivastava G. Expression of HLA class I, beta(2)-microglobulin, TAP1 and IL-10 in Epstein–Barr virus-associated nasal NK/T-cell lymphoma:

implications for tumor immune escape mechanism. *Int J Cancer* 2001; **92**: 692–696.
41. Falcão RP, Rizzatti EG, Saggioro FP, Garcia AB, Marinato AF, Rego EM. Flow cytometry characterization of leukemic phase of nasal NK/T-cell lymphoma in tumor biopsies and peripheral blood. *Haematologica* 2007; **92**: e24–e25.
42. Thome M, Tschopp J. TCR-induced NF-κB activation: a crucial role for Carma1, Bcl10 and MALT1. *Trends Immunol* 2003; **24**: 419–424.
43. Tian MT, Gonzalez G, Scheer B, DeFranco AL. Bcl10 can promote survival of antigen-stimulated B lymphocytes. *Blood* 2005; **106**: 2105–2112.
44. Hara H, Ishihara C, Takeuchi A, Imanishi T, Xue L, Morris SW, *et al*. The adaptor protein CARD9 is essential for the activation of myeloid cells through ITAM-associated and Toll-like receptors. *Nature Immunol* 2007; **8**: 619–629.
45. Wang D, You Y, Lin PC, Xue L, Morris SW, Zeng H, *et al*. Bcl10 plays a critical role in NF-κB activation induced by G protein-coupled receptors. *Proc Natl Acad Sci U S A* 2007; **104**: 145–150.
46. Isaacson P, Du M. MALT lymphoma: from morphology to molecules. *Nature Rev Cancer* 2004; **4**: 644–653.
47. Franco R, Camacho FI, Caleo A, Staibano S, Bifano D, Renzo AD, *et al*. Nuclear bcl10 expression characterizes a group of ocular adnexa MALT lymphomas with shorter failure-free survival. *Mod Pathol* 2006; **19**: 1055–1067.
48. Mak TW, Saunders ME. *The Immune Response: Basic and Clinical Principles*. Elsevier: Boston, 2006; 477–479.
49. Franzoso G, Bours V, Azarenko V, Park S, Tomita-Yamaguchi M, Kanno T, *et al*. The oncoprotein Bcl-3 can facilitate NF-κB-mediated transactivation by removing inhibiting p50 homodimers from select κB sites. *EMBO J* 1993; **12**: 3893–3901.
50. McKeithan TW, Takimoto GS, Ohno H, Bjorling VS, Morgan R, Hecht BK, *et al*. BCL3 rearrangements and t(14;19) in chronic lymphocytic leukemia and other B-cell malignancies: a molecular and cytogenetic study *Genes Chromosomes Cancer* 1997; **20**: 64–72.
51. Ye H, Gesk S, Martin-Subero J, Nader A, Du M, Siebert R. BCL10 gene amplification associated with strong nuclear BCL10 expression in a diffuse large B cell lymphoma with IGH–BCL2 fusion. *Haematologica* 2006; **91**: e81–82.
52. Lobry C, Lopez T, Israël A, Weil R. Negative feedback loop in T cell activation through IκB kinase-induced phosphorylation and degradation of Bcl10. *Proc Natl Acad Sci U S A* 2007; **104**: 908–913.

SUPPORTING INFORMATION ON THE INTERNET

The following supporting information may be found in the online version of this article.

Table S1. List of the antibodies used in the study.

Table S2. Sequences of the primers used for semi-quantitative RT-PCR in the study.

Table S3. Sequences of the primers used for quantitative real-time RT-PCR in the study.

Table S4. shRNA sequences for BCL10 and BCL3 used in the study.

NOTE *Bacteriology*

Differential Detection of Hemotropic *Mycoplasma* Species in Cattle by Melting Curve Analysis of PCR Products

Ikuo NISHIZAWA[1)], Makoto SATO[1)], Masatoshi FUJIHARA[1)], Shigeru SATO[2)] and Ryô HARASAWA[1)]*

[1)]*Departments of Veterinary Microbiology and* [2)]*Clinical Veterinary Medicine, School of Veterinary Medicine, Faculty of Agriculture, Iwate University, Morioka, Iwate 020–8550, Japan*

(Received 3 August 2009/Accepted 26 August 2009/Published online in J-STAGE 5 November 2009)

ABSTRACT. We developed a real-time PCR procedure followed by melting curve analysis using the green fluorescence dye SYBR Green I for rapid detection and differentiation of hemplasmas in cattle. Analysis of the melting temperature (*Tm*) of the PCR products allowed for differentiation of the 2 bovine hemoplasmas, *Mycoplasma wenyonii* and a provisional species, '*Candidatus* Mycoplasma haemobos' (a synonym of '*Candidatus* M. haemobovis'). The *Tm* (mean ± S.E.) of the PCR products from the bovine hemoplasmas were 82.04 ± 0.27°C for *M. wenyonii* and 86.98 ± 0.12°C for '*Candidatus* M. haemobos' in the melting experiments. The protocol described in the present study can decrease the time to results by simultaneous detection and differentiation of the two hemoplasmas in cattle. By using this protocol, we examined hemoplasma prevalence in 109 cattle in Miyagi Prefecture and found that 25 (22.9%) were infected with *M. wenyonii*, 67 (61.5%) were infected with '*Candidatus* M. haemobos' and 14 (12.8%) were infected with both.

KEY WORDS: hemoplasma, Mycoplasma haemobos, *Mycoplasma wenyonii*.

J. Vet. Med. Sci. 72(1): 77–79, 2010

In cattle (*Bos taurus*), two distinct hemotropic mycoplasmas (also known as hemoplasmas) have been identified, *Mycoplasma wenyonii* (formerly *Eperythrozoon wenyonii*) [4] and a provisional species, '*Candidatus* Mycoplasma haemobos (synonym: '*Candidatus* M. haemobovis')' [6, 7]. Hemoplasmas are tiny epierythrocytic bacterial parasites that lack a cell wall like other mycoplasmas and are susceptible to tetracyclines, but have not been cultured *in vitro*. Infection may lead to hemolytic anemia in cattle, but veterinary investigation has been hampered by the lack of appropriate diagnostic procedures. Although most studies have relied on cytological identification of the organisms on blood smears, this method has a low diagnostic sensitivity and cannot distinguish the different species [3]. Furthermore, this diagnostic method may misidentify the hemoplasmas as Howell-Jolly bodies, since they both appear frequently after splenectomy, are associated with anemia and contain DNA. Only recently have real-time PCR-based assays been applied for detection and identification of feline and canine hemoplasma species [8, 9], though no report has been appeared concerning bovine hemoplasmas until now. Distinguishing between these 2 hemoplasmas is necessary because etiological significance has only been established for *M. wenyonii* as a mild anemia in cattle.

There is still little knowledge of the epidemiology of the hemotropic mycoplasmas in cattle [2]. Although *M. wenyonii* in cattle has been shown to exhibit a worldwide geographical distribution, '*Candidatus* M. haemobos' has only been reported in Switzerland (accession numbers EF616467 and EF616468), China (accession number EF460765) and Japan (accession number EU367965).

* CORRESPONDENCE TO: Prof. HARASAWA, R., Department of Veterinary Microbiology, School of Veterinary Medicine, Faculty of Agriculture, Iwate University, Morioka, Iwate 020–8550, Japan.
e-mail: harasawa-tky@umin.ac.jp

In the present study, we demonstrated a rapid method of detecting and distinguishing between the two hemoplasmas in cattle using sensitive real-time PCR with SYBR Green I and melting curve analysis. By using this method, we examined the prevalence and clinical importance of bovine hemoplasma infections in Miyagi Prefecture, Japan.

EDTA-anticoagulated blood samples from 109 cattle in dairy and beef herds in Miyagi Prefecture, Japan, were collected in January 2009 and stored at –80°C for three weeks prior to examination. Information on the clinical diagnoses and ages of all the cattle included in this study were obtained from the Research Unit for Food Animal Internal Medicine & Production Medicine of Iwate University, Japan. The ages of the cattle ranged from seven months to 14 years old.

Total DNA was extracted from 200-*μl* EDTA-anticoagulated blood samples collected from cattle using a QIAamp DNA Blood Mini Kit (Qiagen, Hilden, Germany) according to the manufacturer's instructions. Negative controls consisting of 200 *μl* phosphate-buffered saline were prepared for each batch. Extracted DNA samples were stored at –20°C prior to use.

Conventional PCR was carried out with 50-*μl* reaction mixtures containing 1 *μl* of DNA solution, 0.5 *μl* of TaKaRa LA *Taq*™ (5 units/*μl*), 5 *μl* of 10X LA PCR™ Buffer II, 8 *μl* of 25 mM $MgCl_2$ (final 4.0 mM), 8 *μl* of dNTP mixture (2.5 mM each), 0.2 *μl* of forward primer (5'-ATCTAACATGCCCCTCTGTA-3', equivalent to nucleotide numbers 109 to 128 of '*Candidatus* M. haemobos', or 5'-ACTTTTACGAGGAGGATAGC-3', equivalent to nucleotide numbers 124 to 143 of *M. wenyonii*), reverse primer (5'-GTAGTATTCGGTGCAAACAA-3', equivalent to nucleotide numbers 589 to 608 of '*Candidatus* M. haemobos', or 5'-TGATTAACTCTAGGGAGGCG-3', equivalent to nucleotide numbers 634 to 653 of *M. wenyonii*) (50 pmol/ml each) and water to a final volume of 50 *μl*. After the

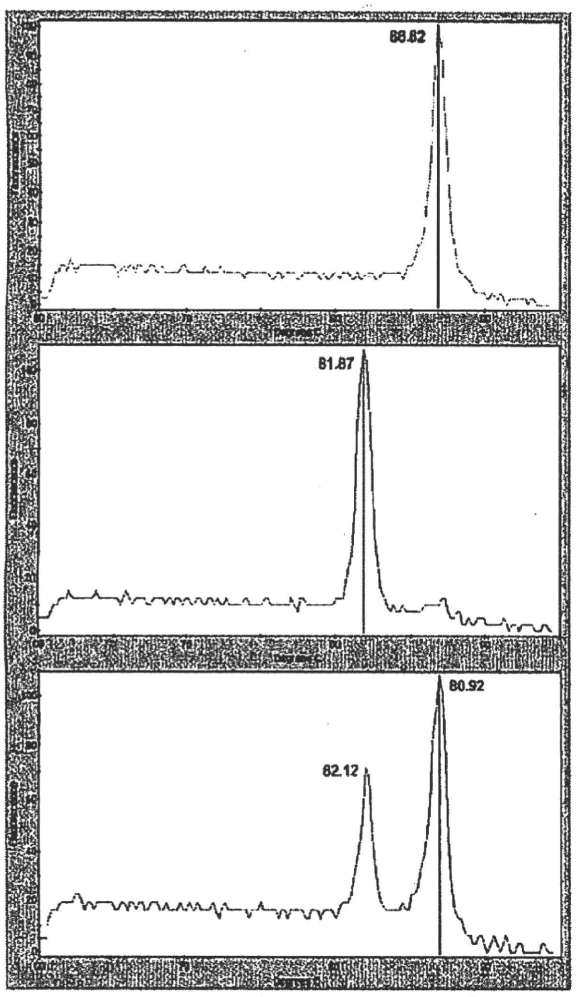

Fig. 1. Melting curves of the PCR products depicted by using SYBR Green I for differentiation. Representative curves for '*Candidatus* M. haemobos' infection (top), *M. wenyonii* infection (middle) and infection with both *M. wenyonii* and '*Candidatus* M. haemobos' (bottom) showing characteristic and distinct peaks at around 87°C and 82°C, respectively, in the melting experiments.

mixture was overlaid with 20 μl of mineral oil, the reaction cycle was carried out 35 times with denaturation at 94°C for 30 sec, annealing at 58°C for 120 sec and extension at 72°C for 60 sec in a thermal cycler. Positive samples were subjected to DNA sequencing for species identification. No polymorphism was evident in the nucleotide sequences.

To detect both mycoplasmas in real-time PCR, specific primers for the 16S rRNA gene of bovine hemoplasmas were originally designed. The forward primer, 5'-ATATTCCTACGGGAAGCAGC-3', equivalent to nucleotide numbers 328 to 347 of *M. wenyonii*, and reverse primer, 5'-ACCGCAGCTGCTGGCACATA-3', equivalent to nucleotide numbers 503 to 522 of *M. wenyonii*, amplified a 195 bp and 173 bp product for *M. wenyonii* and '*Candidatus* M. haemobos', respectively. The nucleotide sequences and sizes bracketed by the primers are peculiar to each hemoplasma. The 22-bp gap in the PCR product from '*Candidatus* M. haemobos' attributes to a genetic marker to distinguish it from *M. wenyonii* in the real-time PCR.

Real-time PCR was performed in a SmartCycler instrument (Cepheid, Sunnyvale, CA, U.S.A.) with SYBR Premix Ex *Taq* (Code #RR041A, TaKaRa Bio., Shiga, Japan). The reaction mixture contained 1 μl of each primer (10 pmol/ml), 12.5 μl of 2X premix reaction buffer and water to volume of 23 μl. Finally, 2 μl of DNA samples as templates were added to this mixture. Amplification was achieved with 40 cycles of denaturation at 95°C for 5 sec, renaturation at 57°C for 20 sec and elongation at 72°C for 15 sec after an initial denaturation at 94°C for 30 sec. Fluorescence readings in a channel for SYBR Green I were taken throughout the experiments. In our experiments, the results of the real-time PCR and conventional PCR were always consistent. The cattle were affected with each hemoplasma irrespective of age. The input amount of DNA, copy number of the target and presence of co-infections with several targets did not influence the *Tm*.

After real-time PCR, a melting experiment was performed from 60 to 95°C at 0.2°C/sec with a smooth curve setting averaging one point. Melting peaks were visualized by plotting the first derivative against the melting temperature (*Tm*) as described previously [1]. The *Tm* was defined as a peak of the curve, and if the highest point was a plateau, then the mid-point was identified as the *Tm*. Since the nucleotide sequences and sizes bracketed by the primers are different between the two species, melting curve analysis of the amplified products allowed for differentiation of these two hemoplasmas. Thus, the variations in the *Tm* depend on sequence variations in the PCR products, which may serve as a differential marker for hemoplasma speciation. No melting peak was evident in the negative cattle.

The *Tm* (mean ± S.E.) of the PCR products from the bovine hemoplasmas were estimated to be 82.04 ± 0.27°C for *M. wenyonii* and 86.98 ± 0.12°C for '*Candidatus* M. haemobos' in the melting experiments (Fig. 1). We identified the strains showing a *Tm* above 82.50°C as *M. wenyonii* and a *Tm* below 86.75°C as '*Candidatus* M. haemobos'. Of the 109 cattle, 25 (22.9%) were infected with *M. wenyonii*, 67 (61.5%) were infected with '*Candidatus* M. haemobos' and 14 (12.8%) were infected with both. There were a few samples showing a *Tm* between the ranges for *M. wenyonii* and '*Candidatus* M. haemobos'. Positive controls were prepared by mixing positive blood samples for the two different hemoplasmas.

The hemoplasma-infected cattle in the present study did not exhibit clinical signs, such as anemia, attributable to hemoplasmosis. The hematocrit values ranged from 22 to 55% in the PCR-positive cattle. Hemoplasma infections in cattle were first recognized in Swiss dairy cattle with hemolytic anemia [2]. In our study, no significant association was found between the infection status and anemic syndrome. This may be due to low level infections, which were

suggested by the poor intensity in PCR. As none of the PCR-positive cattle showed signs of severe anemia and all cattle had been presented for reasons unrelated to hemoplasmosis, laboratory parameters were not analyzed in more detail. Although our results indicate a wide distribution of *M. wenyonii* among the cattle population in Miyagi, Japan, without the development of anemic signs, infected animals probably remain chronic carriers after clinical signs have resolved. Thus, persistent infections with hemoplasmas may contribute to the progression of retroviral, neoplastic or immune-mediated diseases [5].

In the present study, we demonstrated a rapid diagnosis procedure for hemoplasma infections in cattle that allows for distinguishing between *M. wenyonii* and '*Candidatus* M. haemobos' infections by using real-time PCR with melting curve analysis of the PCR products.

REFERENCES

1. Harasawa, R., Mizusawa, H., Fujii, M., Yamamoto, J., Mukai, H., Uemori, T., Asada, K. and Kato, I. 2005. Rapid detection and differentiation of the major mycoplasma contaminants in cell cultures using real-time PCR with SYBR Green I and melting curve analysis. *Microbiol. Immunol.* **49**: 859–863.
2. Hofmann-Lehmann, R., Meli, M.L., Dreher, U.M., Gönczi, E., Deplazes, P., Braun, U., Engels, M., Schüpbach, J., Jörger, K., Thoma, R., Griot, C., Stark, K.D.C., Willi, B., Schmidt, J., Kocan, K.M. and Lutz, H. 2004. Concurrent infections with vector-borne pathogens associated with fetal hemolytic anemia in a cattle herd in Switerland. *J. Clin. Microbiol.* **42**: 3775–3780.
3. Kemming, G.I., Messick, J.B., Enders, G., Boros, M., Lorenz, B., Muenzing, S., Kisch-Wedel, H., Mueller, W., Hahmann-Mueller, A., Messmer, K. and Thein, E. 2004. *Mycoplasma haemocanis* infection—a kennel disease? *Comp. Med.* **54**: 404–409.
4. McAuliffe, L., Lawes, J., Bell, S., Barlow, A., Ayling, R. and Nicholas, R. 2006. The detection of *Mycoplasma* (formerly *Eperythrozoon*) *wenyonii* by 16S rDNA PCR and denaturing gradient gel electrophoresis. *Vet. Microbiol.* **117**: 292–296.
5. Messick, J.B. 2004. Hemotrophic mycoplasmas (hemoplasmas): a review and new insights into pathogenic potential. *Vet. Clin. Pathol.* **33**: 2–13.
6. Tagawa, M., Matsumoto, K. and Inokuma, H. 2008. Molecular detection of *Mycoplasma wenyonii* and '*Candidatus* Mycoplasma haemobos' in cattle in Hokkaido, Japan. *Vet. Microbiol.* **132**: 177–180.
7. Uilenberg, G 2009. '*Candidatus* Mycoplasma haemobos'. *Vet. Microbiol.* **138**: 200–201.
8. Wengi, N., Willi, B., Boretti, F.S., Cattori, V., Riond, B., Meli, M.L., Reusch, C.E., Lutz, H. and Hofmann-Lehmann, R. 2008. Real-time PCR based prevalence study, infection follow-up and molecular characterization of canine hemotropic mycoplasmas. *Vet. Microbiol.* **126**: 132–141.
9. Willi, B., Boretti, F.S., Meli, M.L., Bernasconi, M.V., Casati, S., Hegglin, D., Puorger, M., Neimark, H., Cattori, V., Wengi. N., Reusch, C.E., Lutz, H. and Hofmann-Lehmann, R. 2007. Real-time PCR investigation of potential vectors, reservoirs and shedding patterns of feline hemotropic mycoplasmas. *Appl. Environ. Microbiol.* **73**: 3798–3802.

NOTE *Bacteriology*

Variation of Genes Encoding GGPLs Syntheses among *Mycoplasma fermentans* Strains

Masatoshi FUJIHARA[1,2], Noriko ISHIDA[3], Kozo ASANO[3], Kazuhiro MATSUDA[4], Nobuo NOMURA[4], Yoshihiro NISHIDA[5] and Ryô HARASAWA[1,2]*

[1]*Department of Veterinary Microbiology, Faculty of Agriculture, Iwate University, Morioka, Iwate 020–8850,* [2]*Department of Applied Veterinary Science, The United Graduate School of Veterinary Sciences, Gifu University, Gifu 501–1193,* [3]*Laboratory of Applied Microbiology, Graduate School of Agriculture, Hokkaido University, Sapporo, Hokkaido 060–0808,* [4]*National Institute of Advanced Industrial Science and Technology, Tokyo 135–0064 and* [5]*Department of Applied Biological Chemistry, Graduate School of Horticulture, Chiba University, Matsudo, Chiba 271–8510, Japan*

(Received 18 December 2009/Accepted 27 January 2010/Published online in J-STAGE 5 February 2010)

ABSTRACT. The information of the biosynthesis pathways of *Mycoplasma fermentans* specific major lipid-antigen, named glycoglycerophospholipids (GGPLs), is expected to be some of help to understand the virulence of *M. fermentans*. We examined primary structure of cholinephosphotransferase (*mf1*) and glucosyltransferase (*mf3*) genes, which engage GGPL-I and GGPL-III synthesis, in 20 strains, and found four types of variations in the *mf1* gene but the *mf3* gene in two strains was not detected by PCR. These results may have important implications in virulence factor of *M. fermentans*.

KEY WORDS: cholinephosphotransferase, glucosyltransferase, *Mycoplasma fermentans*.

J. Vet. Med. Sci. 72(6): 805–808, 2010

Mycoplasma fermentans was first isolated from the urogenital tract of patients with ulcerative balanitis several decades ago [19] and then detected from respiratory tract of children with community-acquired pneumonia [4], adults with acute respiratory distress syndrome [10], the joints of patients with rheumatoid and other inflammatory arthritic disorders [5, 6, 8, 21] and so on. Although it was previously assumed that humans were the only natural hosts, *M. fermentans* has been isolated from genital lesions in sheep [15], suggesting a zoonotic aspect of this particular pathogen.

Interest in this organism has recently increased because of its possible role in the pathogenesis of rheumatoid arthritis and reports indicating that this organism may function as a cofactor accelerating the progression of human immunodeficiency virus infection [17]. Although *M. fermentans* is a typical extracellular microorganism able to adhere to human epithelial cells, ultrastructural studies performed with engulfed *M. fermentans* revealed mycoplasmas within membrane-bound vesicles [24, 25].

In mycoplasmas, adherence is the major virulence factor, and adherence-deficient mutants are avirulent [2, 18]. It seems that *M. fermentans* utilizes at least two surface components for adhesion to HeLa cells, a protease-sensitive surface protein, apparently the lipoprotein recently described [23], and a phosphocholine-containing glycolipid. Phosphocholine-containing lipids were detected in all *M. fermentans* strains tested by Ben-Menachem *et al.* [3].

Matsuda *et al.* have identified several alkali labile glycophospholipids designated as glycoglycerophospholipids (GGPLs) [13]. Of them, GGPL-I and GGPL-III are expressed in *M. fermentans* specifically, and these lipid-antigens are the major lipid-antigens of *M. fermentans* [14]. The structures of GGPL-I and GGPL-III were identified as 6'-O-phosphocholine-α-glucopyranosyl-(1'-3)-1,2-diacylglycerol and 1'-phosphocholine-2'-amino dihydroxypropane-3'-phospho-6'-α-glucopyranosyl-(1'3)-1,2-diacylglycerol, respectively [12, 13], and GGPLs have been chemically synthesized by Nishida *et al.* [16].

Based on unique structures and bioactivities, GGPLs have been considered as a hypothetical factor in the pathogenesis of *M. fermentans* [11]. Because GGPLs have strong immunogenicity, they may play roles as immunodisturbing agents in cell functions such as inflammation and cell differentiation [22]. GGPL-III antigens were detected in synovial tissues from RA patients and significantly induced TNF-α and IL-6 production from peripheral blood mononuclear cells, and also proliferation of synovial fibroblasts [9].

The information of the biosynthesis pathways of relative compounds of GGPLs is expected to contribute to identification of those of GGPLs, and Ishida *et al.* determined one of the putative GGPL-I biosynthetic genes, according to whole genome analysis of *M. fermentans* PG18 [7]. In the present study, we examined the presence of cholinephosphotransferase (*mf1*) gene and glucosyltransferase (*mf3*) gene, which engage GGPL-I and GGPL-III synthesis, in human mycoplasma species as well as in 20 strains of *M. fermentans*.

M. fermentans strains used in this study are listed in Table 1. Other human mycoplasmas examined include *M. genitalium* G37, *M. pneumoniae* Mac, *M. pneumoniae* FH, *M. penetrans* GTU, *M. orale* CH19299, *M. buccale* CH20247, *M. primatum* HRC92, and *M. hominis* PG21. *M. fermentans* strains were obtained from Dr. Tsuguo Sasaki of the National Institute for Infectious Disease, Tokyo, Japan and

* CORRESPONDENCE TO: Prof. HARASAWA, R., Department of Veterinary Microbiology, School of Veterinary Medicine, Faculty of Agriculture, Iwate University, Morioka 020–8550, Japan.
e-mail: harasawa-tky@umin.ac.jp

Table 1. Origin of *M. fermentans* strains and *mf1*, *mf3*, *MCGp* sequence type and PCR type based on the major part of the IS*1550* element

Origin	Strain	Year of isolation	*mf1* sequence	*mf3* sequence	IS*1550* PCR type (25)
Genital ulcer	PG18^T	1955	A	+	B
Rheumatoid	KL4	1990	D	+	A
Arthritis	KL8	1990	D	+	B
Joint fluid	GIM	1995	D	+	A
Leukemic bone	E10	1960–1969	D	+	A
marrow	K7	1960–1969	D	+	A
	Z62	1960–1969	D	+	A
Urethral isolate	BRO	1990	D	+	A
AIDS patients					
Urine	#5	1995	C	+	B
Urine	#29	1995	D	+	B
Blood	AOU	1990	D	+	A
Respiratory	M39	1990–1995	A	+	B
tract	M51	1990–1995	D	+	B
	M52	1990–1995	B	+	B
	M64	1990–1995	D	–	B
	M70	1990–1995	D	+	B
	M73	1990–1995	D	–	B
Cell culture	A6	1982–1992	D	+	B
	C5	1982–1992	D	+	B
	2059	1982–1992	D	+	A
	28AC	1982–1992	D	+	B

they include strains KL4, KL8 (from rheumatoid arthritis), GIM (from human joint), E10, K7, Z62 (from bone marrow of leukaemic patients), BRO (from human urethral), #5, #29 (from urine deposits from AIDS patients), AOU (from blood of an AIDS patient), M39, M51, M52 M64, M70, M73 (from human respiratory tract), 2059, 28AC, A6 and C5 (from cell culture). The *mf1* and *mf3* were PCR-amplified from *M. fermentans* genome. Briefly 1 μl of broth cultures (approximately 10^6 cfu/m*l*) were diluted in 1 m*l* of water and heated at 95°C for 3 min for lysis of mycoplasma cells. Mycoplasma lysate (5 μl) was directly added into 45 μl of the PCR master mixture consisting of 1 unit of KOD plus DNA polymerase (TOYOBO, Osaka, Japan), 5 μl of 10 × PCR buffer, 5 μl of 2 mM deoxynucleoside triphosphates, 75 nmol of $MgSO_4$, and 10 pmol of each primer, combination of mf1F (5'-ATAATAAAAACTATGAATGA-3') and mf1R (5'-CTATTTGTCATTTTTCTT-3'), or mf3F (5'-ATGATATGAAAGTTTTTTGTAAAAAAGAAAGG-3') and mf3R (5'-TTATTTTTTATAATGTTCAATAATTT-TTTTGTATTT-3'). Amplification was done under the following conditions; 30 cycles of 94°C for 40 sec, 50°C for 90 sec, and 68°C for 2 min after 94°C for 2 min. *mf1* and *mf3* amplified products (777 and 1,221 bp respectively) were sent to a reference laboratory (TaKaRa Custom Services, Shiga, Japan) for DNA sequencing.

In our study, *mf1* and *mf3* are thought to be *M. fermentans* specific genes because they were not amplified in case of other human mycoplasmas (*M. genitalium* G37, *M. pneumoniae* Mac, *M. pneumoniae* FH, *M. penetrans*, *M. orale*, *M. buccale* CH20247, *M. primatum* HRC92, *M. hominis* PG21).

The sequence data of *mf1* gene were deposited to the international DNA databases under the accession number AB480306 ~ AB480325. Although the *mf1* gene was shown to be conservative in 20 strains of *M. fermentans* by PCR, *mf3* gene was not amplified in two strains, M64 and M73, among these 20 strains examined. Besides, the *mf1* and *mf3* genes were not evident in other human *Mycoplasma* species by specific PCR, suggesting that these two genes are unique to the *M. fermentans* species. Nucleotide sequences of *mf3* gene in the 20 *M. fermentns* strains were identical, but those of *mf1* gene showed a minor variation causing some amino acid substitutions, and categorize A, B, C, and D types for descriptive purposes (Fig. 1). These amino acid changes may be responsible for enzymatic activity of cholinephosphotransferase in *M. fermentans*. In addition, although the *mf3* gene was not amplified from strains M64 and M73, the reason was currently unknown since defection of glucosyltransferase in these strains was not examined in the present study. These diversities in enzymes may engage specific major lipid-antigen syntheses, and also influence immunogenic potential and RA pathogenesis. No significant homology to the *mf3* gene was apparent in other prokayotes in databases, supporting that the GGPLs are unique to *M. fermentans*. Currently recombinant enzymes, based on the nucleotide sequences of the enzyme genes from PG18 strain of *M. fermentans*, have been successfully expressed in *Escherichia coli* [7]. PG18, a type strain of *M. fermentans*, has been shown particularly unique among *M. fermentanss* strains [20]. The difference of *mf1* posttranslational amino-acid sequence may have influenced the activity of choline phosphotransferase, and concern GGPL-I

Fig. 1. The part of *mf1* DNA (top) and posttranslational amino-acid sequence data (bottom) of *M. fermentans* PG18 reference strain. The 20 strains tested were differentiate into four types A including PG18 and M39, B including M52, C including #5 and D including the other strains.

antigenicity, so studies on not only PG18 strain but also on other strains will become increasingly important. In addition, all strains presenting A type in IS*1550* PCR pattern were D type in *mf1* and detected *mf3*, however, there seems to be poor correlation among IS*1550*, *mf1* and *mf3*.

In conclusion, our genetic analysis on the 20 strains of *M. fermentans* showed four variations in *mf1* posttranslational amino-acid sequence but undetected *mf3* gene in two strains. Our results may have important implications for the virulence of *M. fermentans* especially in RA pathogenesis.

REFERENCES

1. Afshar, B., Pitcher, D., Nicholas, R. A. and Miles, R. J. 2008. An evaluation of PCR methods to detect strains of Mycoplasma fermentans. *Biologicals* **36**: 117–121.
2. Baseman, J. B., Lange, M., Criscimagna, N. L., Iron, J. A. and Thomas, C. A. 1995. Interplay between mycoplasmas and host target cells. *Microb. Pathog.* **19**: 105–116.
3. Ben-Menachem, G., Zähringer, U. and Rottem, S. 2001. The phosphocholine motif in the cell membrane of M. fermentans strains. *FEMS Microbiol. Lett.* **199**: 137–141.
4. Cassell, G. H., Yanez, A., Duffy, L. B., Moyer, J., Cedillo, L., Hammerschlag, M. R., Rank, R. G. and Glass, J. I. 1994. Detection of *Mycoplasma fermentans* in respiratory tract of children with pneumoniae. *IOM Lett.* **3**: 456.
5. Haier, J., Nasralla, M., Franco, A. R. and Nicolson, G. L. 1999. Detection of mycoplasmal infections in blood of patients with rheumatoid arthritis. *Rheumatology (Oxford)* **38**: 504–509.
6. Horowitz, S., Yevinson, B. and Horowitz, J. 2000. *Mycoplasma fermentans* in rheumatoid arthritis and other inflammatory arthritides. *J. Rheumatol.* **27**: 2747–2753.
7. Ishida, N., Irikura, D., Matsuda, K., Sato, S., Sone, T., Tanaka, M. and Asano, K. 2009. Molecular cloning and expression of a novel cholinephosphotransferase involved in glycoglycerophospholipid biosynthesis of *Mycoplasma fermentans*. *Curr. Microbiol.* **58**: 535–540.
8. Johnson, S. M., Sidebottom, D., Bruckner F. and Collins, D. 2000. Identification of *Mycoplasma fermentans* in synovial fluid samples from arthritis patients with inflammatory disease. *J. Clin. Microbiol.* **38**: 90–93.
9. Kawahito, Y., Ichinose, S., Sano, H., Tsubouchi, Y., Kohno, M., Yoshikawa, T., Tokunaga, D., Hojo, T., Harasawa, R., Nakano, T. and Matsuda, K. 2008. *Mycoplasma fermentans* glycolipid-antigen as a pathogen of rheumatoid arthritis. *Biochem. Biophys. Res. Commun.* **369**: 561–566.
10. Lo, S. C., Wear, D. J., Green, S. L., Jones, P. G. and Legier, J. F. 1993. Adult respiratory distress syndrome with or without systemic disease associated with infections due to *Mycoplasma fermentans*. *Clin. Infect. Dis.* **17**: S259–263.
11. Matsuda, K. 2004. Phosphocholine-containing glycoglycerolipids of *Mycoplasma fermentans* as a pathogen of rheumatoid arthritis: possible role of *Mycoplasma fermentans* GGPLs in the pathogenesis of neuroendocrine-immune abnormalities, *Recent Res. Dev. Neurosci.* **1**: 15–23.
12. Matsuda, K., Ishizuka, I., Kasama, T., Handa, S., Yamamoto, N. and Taki, T. 1997. Structure of a novel phosphocholine-containing aminoglycoglycerolipid of Mycoplasma fermentans. *Biochim. Biophys. Acta* **1349**: 1–12.
13. Matsuda, K., Kasama, T., Ishizuka, I., Handa, S., Yamamoto, N. and Taki, T. 1994. Structure of a novel phosphocholine-containing glycoglycerolipid from *Mycoplasma fermentans*. *J. Biol. Chem.* **269**: 33123–33128.
14. Matsuda, K., Li, J. L., Harasawa, R. and Yamamoto, N. 1997. Phosphocholine-containing glycoglycerolipids (GGPL-I and GGPL-III) are species-specific major immunodeterminants of *Mycoplasma fermentans*. *Biochem. Biophys. Res. Commun.* **233**: 644–649.
15. Nicholas, R. A. J., Greig, A., Baker, S. E., Ayling, R. D., Heldtander, M., Johansson, K. E., Houshaymi, B. M. and Miles, R. J. 1998. Isolation of *Mycoplasma fermentans* from a sheep. *Vet. Rec.* **142**: 220–221.
16. Nishida, Y., Ohrui, H., Meguro, H., Ishizawa, M., Matsuda, K., Taki, T., Handa, S. and Yamamoto, N. 1994. Synthesis and absolute configuration of 6-o-phosphocholine-α-D-glucopyranosyl glycerolipid isolated from HTLV-I-infected cell lines. *Tetrahedron Lett.* **35**: 5465–5468.
17. Rosengarten, R., Citti, C., Glew, M., Lischewski, A., Droesse, M., Much, P., Winner, F., Brank, M. and Spergser, J. 2000. Host-pathogen interactions in mycoplasma pathogenesis: virulence and survival strategies of minimalist prokaryotes. *Int. J. Med. Microbiol.* **290**: 15–25.
18. Rottem, S. and Naot, Y. 1998. Subversion and exploitation of host cells by mycoplasmas. *Trends Microbiol.* **6**: 436–440.
19. Ruiter, M. and Wentholt, H. M. M. 1952. The occurrence of a pleuropneumonia-like organism in the fuso-spirillary infections of the human genital mucosa. *J. Invest. Dermatol.* **18**: 313–323.
20. Sasaki, T., Sasaki, Y., Kita, M., Suzuki, K., Watanabe, H. and Honda, M. 1992. Evidence that Lo's mycoplasma (*Mycoplasma fermentans* incognitus) is not a unique strain among Mycoplasma fermentans strains. *J. Clin. Microbiol.* **30**: 2435–

2440.

21. Schaeverbeke, T., Gilroy, C. B., Beébéar, C., Dehais, J. and Taylor-Robinson, D. 1996. *Mycoplasma fermentans*, but not *Mycoplasma penetrans*, detected by PCR assays in synovium from patients with rheumatoid arthritis and other rheumatic disorders. *J. Clin. Pathol.* 49: 824–828.
22. Schutze, S., Potthoff, K., Machleidt, T., Berkovic, D., Wiegmann, K. and Kronke, M. 1992. TNF activates NF-kappa B by phosphatidylcholine-specific phospholipase C-induced "acidic" sphingomyelin breakdown. *Cell* 71: 765–776.
23. Spencer, A. L. and Wise, K. S. 2002. Identification and functional mapping of the *Mycoplasma fermentans* P29 adhesin. *Infect. Immun.* 70: 4925–4935.
24. Stadtlander, C. T., Watson, H. L., Simecka, J. W. and Cassell, G. H. 1993. Cytopathogenicity of *Mycoplasma fermentans* (including strain incognitos). *Clin. Infect. Dis.* 17: 289–301.
25. Taylor-Robinson, D., Davies, H. A., Sarathchandra, P. and Furr, P. M. 1991. Intracellular location of mycoplasmas in cultured cells demonstrated by immunocytochemistry and electron microscopy. *Int. J. Exp. Pathol.* 72: 705–714.

FULL PAPER *Bacteriology*

Nitric Oxide Causes Anoikis through Attenuation of E-Cadherin and Activation of Caspase-3 in Human Gastric Carcinoma AZ-521 Cells Infected with *Mycoplasma hyorhinis*

Hisato OBARA[1,2,3] and Ryô HARASAWA[1,3]*

[1]*Department of Veterinary Microbiology, School of Veterinary Medicine, Faculty of Agriculture, Iwate University, Morioka 020–8550,* [2]*Will Animal Hospital, Sendai, Miyagi 983-0826 and* [3]*Department of Applied Veterinary Science, The United Graduate School of Veterinary Sciences, Gifu University, Gifu 501–1193, Japan*

(Received 18 December 2009/Accepted 10 February 2010/Published online in J-STAGE 24 February 2010)

ABSTRACT. *Mycoplasma hyorhinis* (*M. hyorhinis*) infection leads cultured cells to various biological alterations in cell metabolism including apoptosis. Apoptosis induced by *M. hyorhinis* has mainly been considered to be due to mycoplasmal endonucleases. We previously reported that apoptosis in a human carcinoma cell line AZ-521 infected with *M. hyorhinis* was enhanced by addition of L-ascorbic acid to cell cultures. Since both L-ascorbic acid addition and *M. hyorhinis* infection activated cellular iNOS, we examined the hypothesis that nitric oxide (NO) exerts an apoptotic effect on *M. hyorhinis*-infected cells and down-regulates E-cadherin. In this study, we showed that *M. hyorhinis* infection activates iNOS mRNA synthesis, NO production, and caspase-3 activity and attenuates E-cadherin mRNA synthesis by quantitative real-time PCR, Griess assay and fluorescence caspase-3 detection. L-NAME decreased the numbers of apoptotic cells through inhibition caspase-3 activity. Our results indicate that NO causes anoikis throughout attenuation of E-cadherin and activation of caspase-3 in human gastric carcinoma cell line AZ-521 cells infected with *M. hyorhinis*.

KEY WORDS: anoikis, apoptosis, E-cadherin, *Mycopalsma hyorhinis*, nitric oxide.

J. Vet. Med. Sci. 72(7): 869–874, 2010

Mycoplasmas are the smallest self-replicating prokaryotes, lack rigid cell walls and belong to the class *Mollicutes* [25]. Most mycoplasma species inhabit plants, insects, animals and humans as normal flora in their hosts. Although some are pathogenic, many possess an opportunistic character [22].

Mycoplsma hyorhinis (*M. hyorhinis*) causes polyserositis [7], otitis media [19], arthritis [12] and pneumonia [1] in piglets. These mycoplasmal infections are responsible for economical losses on swine farms. *M. hyorhinis* is also a major and serious contaminant in cell cultures [2]. In addition, it has been demonstrated in human gastric carcinoma tissues [26], and it has been suggested that lipoprotein P37 of *M. hyorhinis* contributes to invasiveness and metastasis of the tumor cells [5, 14].

M. hyorhinis infection has a significant impact on the physiology of cell cultures, including apoptosis, which has previously been explained by mycoplasmal endonucleases [23], production of nitric oxide (NO) by activating cellular inducible NO synthase (iNOS) and production of reactive oxygen species (ROS) in various cell lines [13]. NO is a multifunctional molecule involved in a variety of physiological and pathological processes [17]. While low concentrations of NO can protect cells from apoptosis, excess NO promotes cell death in various cell types [3].

Apoptosis is characterized morphologically by cell shrinkage and chromatin condensation and biochemically by DNA laddering [30]. Detection of caspase activity is a useful assay for apoptosis. The caspase family participates in a series of reactions that are trigged in proapototic signals and result in the cleavage of substrates, and caspases are synthesized as inactive precursors that undergo proteolytic maturation upon apoptotic stimulation [27].

Adhesion of cells to the extracellular matrix (ECM) is important as detachment from the matrix triggers apoptosis referred to as anoikis [7]. It has recently been reported that anoikis is caspase-3 dependent [6]. Epithelial cadherin (E-cadherin) is the prime mediator of intracellular adhesion [28]. Our preliminary examination suggested marked down-regulation of E-cadherin expression in AZ521 cells infected with *M. hyorhinis* based on a microarray analysis (unpublished data). Therefore, we hypothesized that excessive NO produced by *M. hyorhinis* infection leads to anoikis in AZ-521 cells.

We previously reported that apoptosis in human carcinoma cell line AZ-521 infected with *M. hyorhinis* was enhanced by addition of L-ascorbic acid (AsA) to the cell cultures [21]. Since *M. hyorhinis* infection and/or AsA addition enhance iNOS activity [20], we proposed a hypothesis that *M. hyorhinis* infection results in the presence of another external apoptotic pathway including the NO pathway. The aim of the present study was to obtain insights into the role of NO in cell adhesion-dependent apoptosis in cells infected with *M. hyorhinis*.

In the present study, we examined the role of NO in apoptosis induced by *M. hyorhinis* infection. We used a general competitive inhibitor of NOS, N^{ω}-nitro-L-arginine methyl ester (L-NAME), to measure NO based on the Griess assay

* CORRESPONDENCE TO: Prof. HARASAWA, R., Department of Veterinary Microbiology, School of Veterinary Medicine, Faculty of Agriculture, Iwate University, Morioka 020–8550, Japan.
e-mail: harasawa@iwate-u.ac.jp

and analyzed iNOS and E-cadherin expression by real-time PCR (RT-PCR) and caspase-3 detection. This study may also promote understanding of the mechanism of piglet diseases caused by *M. hyorhinis*.

MATERIALS AND METHODS

Cell cultures: Human gastric carcinoma cell line AZ-521 was obtained from the Health Science Research Resources Bank (Osaka, Japan) and was maintained in Dulbecco's modified Eagle's minimum essential medium (DMEM) supplemented with 10% fetal calf serum (Gibco BRL, Grand Island, NY, U.S.A.), 1% penicillin and streptomycin (100 U/ml) at 37°C in a humidified 5% CO_2 atmosphere. To minimize the pH change by L-NAME (Nacalai Tesque Inc., Kyoto, Japan) addition to the cell culture, 4-(2-hydroxyethyl)-1-piperazineethanesulfonic acid (HEPES) buffer (pH 7.5) was added to the DMEM at a final concentration of 50 mM. The cell culture was tested for the absence of mycoplasma contamination by using a PCR Mycoplasma Detection Set (TaKaRa-Bio, Shiga, Japan) according to the manufacturer's instructions. The cells were seeded into chamber flasks at 8.5×10^5 cells per chamber (Asahi Techno Glass, Tokyo, Japan).

Five hundred μM of L-NAME were added to the final concentration as indicated. The vehicle for L-NAME was distilled water, and distilled water was used as a control. Addition of distilled water or 500 μM of L-NAME to AZ-521 cells did not produce any differences in this study (data not shown) using trypan blue staining after 30 hr of incubation in order to monitor the cytotoxic effect of distilled water [16]. The reagents were freshly prepared and dissolved in distilled water before pretreatment.

M. hyorhinis strain and its growth conditions: The BTS-7 strain of *M. hyorhinis* was used in present study. *M. hyorhinis* was grown at 37°C in PPLO broth (Difco, Detroit, MI, U.S.A.) supplemented with 20% horse serum (Gibco BRL, Grand Island, NY, U.S.A.), 5% fresh yeast extract (ICN Biomedicals, Inc., OH, U.S.A.) and 0.5% glucose instead of bacteriological mucin [15]. The propagation of *M. hyorhinis* was expressed as Colony-forming units (CFU). *M. hyorhinis* was inoculated into the AZ-521 cell culture at a multiplicity of infection (MOI) of 10^3 after seeding the cells into Chamber Slide II wells (Asahi Techno Glass, Tokyo, Japan). *M. hyorhinis* grown in PPLO broth containing 500 μM of L-NAME and HEPES (pH 7.5) was calculated after 30 hr of incubation at 37°C. Viability of the AZ-521 cells and *M. hyorhinis* strain were not affected by incubation with distilled water or 500 μM of L-NAME after 30 hr post-inoculation (data not shown).

Quantitative RT-PCR for iNOS and E-cadherin mRNA transcription: Total RNA was extracted from AZ-521 cells inoculated with *M. hyorhinis*, after 20, 24 and 28 hr using RNA-Bee™ (Tel-Test, Inc., Pearland, TX, U.S.A.), precipitated by isopropanol and dissolved in diethyl pyrocarbonate-treated water.

Similarly, total RNA was extracted from AZ-521 cells inoculated with *M. hyorhinis* and treated or not treated with 100, 250 and 500 μM of L-NAME after 24 and 28 hr. The RNA was transcribed with *Moloney murine leukemia* virus reverse transcriptase (Invitrogen, Carlsbad, CA, U.S.A.) according to the manufacturer's instructions. First-strand complementary DNA was quantitatively analyzed for the expression of iNOS and E-cadherin gene in a SmartCycler instrument (Cepheid, Sunnyvale, CA, U.S.A.) with TaKaRa Ex *Taq* R-PCR (TakaRa Bio, Shiga, Japan). The reaction mixture contained 1 μl of each primer (10 pmol/μl), 2.5 μl of 10 × reaction buffer, 20 nmol of each deoxynucleotide, 0.25 μl of 250 mM $MgCl_2$, 0.2 μl (5 U/μl) TaKaRa Ex *Taq* HS DNA polymerase (TaKaRa Bio, Shiga, Japan), 2.5 μl of 1:3,000 SYBR Green I (TaKaRa Bio, Shiga, Japan) and water to a volume of 23 μl. Finally, 2 μl of RNA as a template was added to this mixture. The conditions of amplification were as follows: after initial melting at 94°C for 2 min, amplification was performed with 40 cycled of 94°C for 10 sec, 55°C for 30 sec and 72°C for 30 sec. The primer sequences used were as follows: 5'- CGG TGC TGT ATT TCC TTA CGA GGC GAA GAA GG-3', forward, and 5'-GGT GCT GCT TGT TAG GAG GTC AAG TAA AGG GC-3', reverse, for iNOS (394 bp) [13]; 5'-AGA ATG ACA ACA AGC CCG AAT-3', forward, and 5'-CGG CAT TGT AGG TGT TCA CA-3', reverse for E-cadherin (132 bp) [4]; and 5'- GTC TTC ACC ACC ATG GAG AAG GCT-3', forward, and 5'-CAT GCC AGT GAG CTT CCC GTT CA-3', reverse, for glyceraldehydes-3-phosphate dehydrogenase (GAPDH; 420 bp) [13]. The amount of target gene transcription was calculated from the standard curves and was normalized using the transcription of the housekeeping GAPDH gene as an internal control. The value for the mock-infected control was scored as one.

Measurement of NO oxidation products, nitrite and nitrate: NO is chemically unstable and undergoes rapid oxidation to nitrite, and cellular components catalyze its further oxidation to nitrate. Therefore, production of NO was determined by measuring the formation of the stable oxidation products of NO, nitrite and nitrate as described previously [10]. After the cells had been infected with *M. hyorhinis* for 20, 24 and 28 hr, total nitrite and nitrate concentrations in the cell culture were determined based on the Griess reaction by using a Total Nitric Oxide Assay Kit (Assay Designs Inc., Ann Arbor, MI, U.S.A.) according to manufacturer's instructions. The cell culture was collected after centrifugation at 1,000 × g for 5 min. The collected supernatant fluid was stored at −80°C until measurement of nitrate. The absorbance was measured at a wavelength of 570 nm in an NJ-2000 multiwell plate reader (InterMed, Tokyo, Japan).

Fluorescent microscopic analysis for apoptotic cell count and caspase-3 activity detection: The AZ-521 cells were examined for apoptotic changes by using a fluorescent dye, Hoechst 33258 (Dojin Chemicals, Kumamoto, Japan). We observed fluorescent nuclei showing apoptotic changes, mainly due to chromatin condensation, at 400 × magnification by using 352 and 461 nm band pass filters for excitation and emission, respectively, on an Eclipse E400 fluorescent

microscope (Nikon, Tokyo, Japan). At 24 and 28 hr post-inoculation, we counted the number fluorescent cells infected with BTS-7 showing apoptotic changes at 400 × magnification in 200 AZ-521 cells each treated with or without 100, 250 or 500 μM of L-NAME. Apoptosis was expressed as the percentage of cells with an apoptotic nuclear morphology in relation to the total cell number.

Furthermore, to detecte caspase-3 activity in AZ-521 cells, we used an APO LOGIX™ FAM-DEVD-FMK Carboxyfluorescein Caspase Detection Kit (Cell Technology Inc., Mountain View, CA, U.S.A.). AZ-521 cells grown in the DMEM containing 500 μM of L-NAME were examined more than 24 and 28 hr after inoculation with *M. hyorhinis*, according to manufacturer's instructions. Caspase-3 activity of AZ-521 cells was examined by counting the number fluorescent cells that were positive for caspase-3 in 200 AZ-521 cells at 400 × magnification.

Statistical analysis: The data was analyzed using analysis of variance (ANOVA) for comparison between groups using StatView ver. 5 (Hulinks Inc., Tokyo, Japan). Differences were accepted as significant values at $P<0.05$. Each test was repeated three times. Data were expressed as mean ± SEM values.

RESULTS

RT-PCR analysis of iNOS and E-cadherin transcription: The transcription levels of iNOS and E-cadherin were examined by using RT-PCR (Fig. 1). At 20, 24 and 28 hr post-inoculation, a significant amount of iNOS mRNA was detected in the *M. hyorhinis*-infected AZ-521 cells. On the other hand, no significant difference in iNOS mRNA transcription was observed in the mock-infected controls at any hour post-inoculation. These results suggested that *M. hyorhinis* induced iNOS mRNA expression in the AZ-521 cells.

Similarly, E-cadherin mRNA transcription was examined in AZ-521 cells treated with or without 100, 250 or 500 μl of L-NAME at 24 and 28 hr post-inoculation (Fig. 2). *M. hyorhinis* infection caused decreases of E-cadherin mRNA transcription at 24 and 28 hr post-inoculation as compared with the mock-infected controls. Also, the amount of E-cadherin mRNA was significantly decreased in the *M. hyorhinis*-infected AZ-521 cells treated with 500 μl of L-NAME at 24 hr and in those treated with 250 and 500 μl of L-NAME at 24 hr and 28 hr post-inoculation. *M. hyorhinis* infection did not alter GAPDH mRNA transcription. These results suggested that *M. hyorhinis* infection attenuates E-cadherin mRNA transcription by NO-dependency in AZ-521 cells.

Measurement of NO oxidation products, nitrite and nitrate: To determine whether or not the expressed iNOS in AZ-521 cells produces NO, NO synthesis was assayed by measuring the accumulation of the NO end products, nitrite and nitrate, in the medium (Fig. 3). At 20 hr post-inocula-

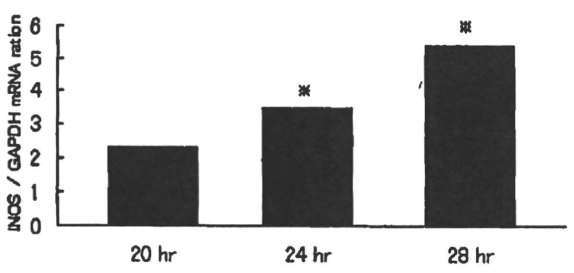

Fig. 1. Expression of iNOS in AZ-521 cells was analyzed by quantitative real-time PCR. The cells were treated with *M. hyorhinis* for 24 and 28 hr. The intensity of iNOS mRNA expression was normalized by that of GAPDH, and the value for mock was estimated as 1. Means ± SEM for 2 separate replications are shown. Statistical significance was determined using ANOVA. * $p<0.05$.

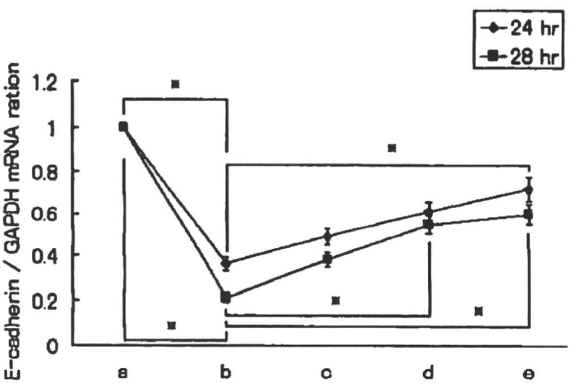

Fig. 2. E-cadherin expression in AZ-521 cells was analyzed by quantitative real-time PCR. The cells were infected with *M. hyorhinis* and treated with (b) no L-NAME, (c) 100, (d) 250 or (e) 500 μM of L-MAME or (a) mock for 24 and 28 hr. The intensity of E-cadherin mRNA expression was normalized by that of GAPDH. The value for mock was set at 1. Means ± SEM for 2 separate replications are shown. Statistical significance was determined using ANOVA. * $p<0.05$.

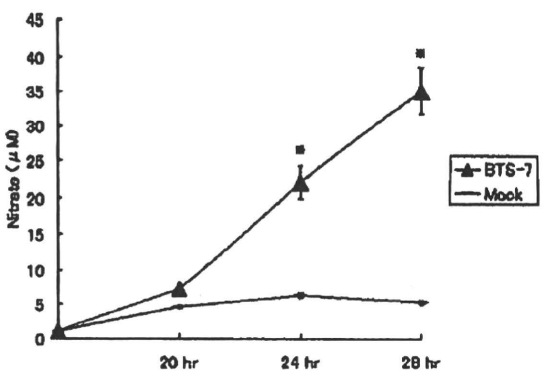

Fig. 3. Nitrate production in AZ-521 cells infected with *M. hyorhinis* at 20, 24 and 28 hr post inoculation. Means ± SEM for two separate replications are shown. Statistical significance was determined using ANOVA. * $p<0.05$.

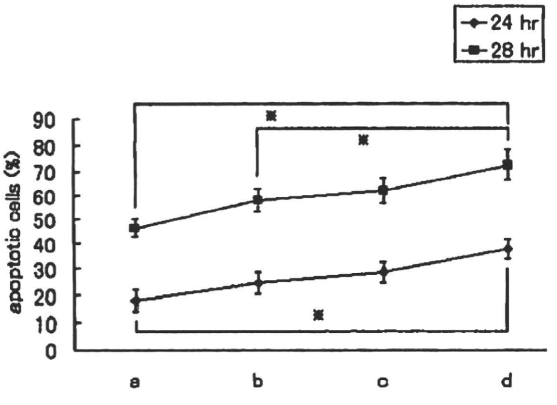

Fig. 4. The effect of L-NAME on *M. hyorhinis*-induced apoptosis in AZ-521 cells. The cells were infected with *M. hyorhinis* treated with (a) 500, (b) 250 or (c) 100 μM of L-MAME or with (d) no L-NAME for 24 and 28 hr. Means ± SEM for 2 separate replications are shown. Statistical significance was determined using ANOVA. * $p<0.05$.

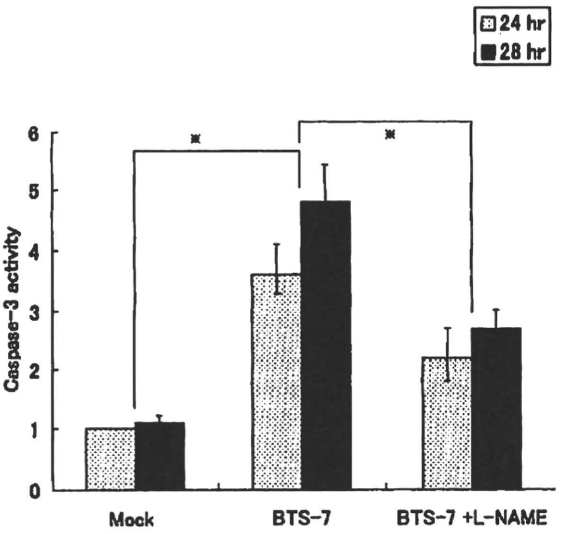

Fig. 5. Caspase-3 activity of AZ-521 cells infected with *M. hyorhinis* at 24 and 28 hr post inoculation. AZ-521 cells were treated with 500 μM of L-NAME. AZ-521 cells infected with *M. hyorhinis* at 24 and 28 hr post inoculation; in the non-treated AZ-521cells, the number of caspase-3 positive cells was scored as 1, and the numbers of caspase-3 positive AZ-521 cells were counted in *M. hyorhinis*-infected cells treated with 500 μM L-NAME or without. Means ± SEM for 2 separate replications are shown. Statistical significance was determined using ANOVA. * $p<0.05$.

tion, no significant NO production was evident among the different *M. hyorhinis*-infected AZ-521 cells or in the mock-infected controls. Together with the augmentation of iNOS mRNA expression, nitrite and nitrate increased in the *M. hyorhinis*-infected AZ-521 cells at 24 and 28 hr post-inoculation compared with the mock-infected controls AZ-521 cells. These results corresponded to the results of the RT-PCR analyses for iNOS expression.

Fluorescent microscopic analysis for apoptotic cell counts and caspase-3 activity detection: The AZ-521 cells were examined for apoptotic changes by using a fluorescent microscope. Addition of 100, 250 and 500 μM L-NAME to AZ-521 cells infected with *M. hyorhinis* at 24 and 28 hr post-inoculation showed that L-NAME significantly inhibited apoptosis depending on the concentrations, except for 100 μM of L-NAME at 28 hr (Fig. 4).

To examine whether caspase-3 was involved in apoptosis induced by BTS-7 infection, we examined caspase-3 activity in AZ-521 cells by using an FAM-DEVD-FMK kit (Fig. 5). *M. hyorhinis*-infected AZ-521 cells showed significant caspase-3 activity at 24 and 28 hr post-inoculation compared with the mock-infected controls. This indicated that *M. hyorhinis* has another apoptotic pathway other than its endonucleases as previously reported [23]. Furthermore, at both 24 and 28 hr after inoculation with 500 μM of L-NAME, *M. hyorhinis*-infected AZ-521 cells were significantly less caspase-3 positive than non-treated *M. hyorhinis*-infected AZ-521 cells. These results suggested that NO produced by AZ-521 cells infected with *M. hyorhinis* plays an important role in activating caspase-3 and finally promoting apoptosis.

DISCUSSION

The present study is the first to provide data showing that the BTS-7 strain of produces excessive amounts of NO and attenuates E-cadherin expression, leading to anoikis.

Two regular apoptotic pathways have previously been identified. The extrinsic pathway is triggered by receptor/ligand interaction such as TNF receptor-1/TNF-alpha [31] and is mediated by "initiator" caspase-8 to the death receptor complex [24]. This leads to activation of "executioner" caspase-3, which can further activate downstream substrates involved in apoptotic changes [27]. In the present study, we showed that caspase-3 activity increased in AZ-521 cells infected by *M. hyorhinis*, and L-NAME-treated AZ-521 cells infected by *M. hyorhinis* had decreased caspase-3 activity as compared with the mock-infected AZ-521 cells (Fig. 5). Activation of caspase-3 is a downstream event in apoptosis and may occur before apoptosis. Thus, the "true" caspase-3 activity may be higher than in this study (at 24 and 28 hr). The more NO increased, the more cellular apoptosis and caspase-3 activity increased.

Different stress situations may alter matrix proteins, and such alteration may affect cell-matrix adhesion [28]. During cell-matrix adhesion, adhesion molecules on cell membrane surfaces recognize their matrix protein receptors as an initial step of adhesion. The present study showed that *M. hyorhinis* infection decreased E-cadherin mRNA expression in AZ-521 cells (Fig. 2). Since E-cadherin is the prime mediator of intracellular adhesion [28], E-cadherin down-regulation means the collapse of cell-matrix adhesion,

occurs anoikis in dependent on caspase-3.

NO can promote or inhibit cell death [3] in various cells depending on the concentration of intracellular NO in combination with the intracellular environment and its interactions with other biological molecules such as oxygen or superoxide. Excess NO induces apoptosis in various cells [3]. Also, NO rapidly reacts with superoxide anion radicals to form peroxynitrite, which is an oxidant substance producing cytotoxic effects in many cells [29]. It is known that peroxynitrite induces apoptosis [29]. Overproduction of NO resulting from *M. hyorhinis* infection may induce a caspase cascade. The present paper presents evidence showing that the unselective NOS inhibitor L-NAME prevented apoptosis induced by *M. hyorhinis* infection (Fig. 4). This suggests that excess amounts of NO or the NO reactant peroxynitrite resulting from *M. hyorhinis* decrease E-cadherin expression (Fig. 2) and lead to anoikis in AZ-521 cells.

M. hyorhinis infection in cell cultures causes diverse biological effects. For example, it has been reported that *M. hyorhinis* infection activates nNOS expression in human neuroblastoma cell line YT-nu [9]. Therefore, it is necessary to ascertain the absence of mycoplasma in cell cultures prior to study [11].

In conclusion, we first showed that *M. hyorhinis* induces anoikis in AZ-521 cells through NO production and E-cadherin down-regulation. Although we have obtained similar results in MDBK cells infected with *M. hyorhinis* (unpublished data), our results await application to other host cell types. Since *M. hyorhinis* is very common in nasal and tracheobronchial secretions of young swine [22], a few of strains of *M. hyorhinis* may induce apoptosis *in vitro*. In fact, we have shown that there is a difference in the amount of induced iNOS mRNA expression, NO production and apoptosis in AZ-521 cells between *M. hyorhinis* strains (data not shown). The difference of virulence to piglets among *M. hyorhinis* strains may depend on the ability to produce NO and induce apoptosis *in vivo*. However, we did not elucidate the relation between pathogenecity to piglets and the difference in ability to produce NO by cells infected with *M. hyorhinis* strains. It might be necessary to confirm whether serious lesion of piglets infected with *M. hyorhinis* presents mainly apoptotic cells. The present study will lend us further understanding of the mechanism of the piglet diseases caused by *M. hyorhinis*. Our results also underline the potential application of NOS inhibitor in the treatment of *M. hyorhinis*-induced swine diseases. However, the molecular mechanism of effect of NO on swine diseases needs further exploration.

REFERENCE

1. Assuncao, P. De, la, Fe, C., Kokotovic, B., Gonzalez, O. and Poveda, J. B. 2005. The occurrence of mycoplasmas in the lungs of swine in Gran Canaria (Spain). *Vet. Res. Commun.* **29**: 453–462.
2. Bölske, G. 1989. Survey of mycoplasma infections in cell cultures and a comparison of detection methods. *Zentralbl. Bakteriol. Mikrobiol. Hyg. [A]* **269**: 331–340.
3. Brune, B., von, Knethen, A. and Sandau, K. B. 1998 Nitric oxide and its role in apoptosis. *Eur. J. Pharmacol.* **351**: 261–272.
4. Chen, M., Fu, Y. Y., Lin, C. Y., Chen, L. M. and Chai, K. X. 2007. Prostasin induces protease-dependent and independent molecular changes in the human prostate carcinoma cell line PC-3. *Biochim. Biophys. Acta* **1773**: 1133–1140.
5. Chmidhauser, C., Dudler, R., Schmidt, T. and Parish, R. W. 1990. A mycoplasmal protein influences tumour cell invasiveness and contact inhibition *in vitro*. *J. Cell Sci.* **95** (*Pt 3*): 499–506.
6. Feng, J., Yang, S., Xu, L., Tian, H., Sun, L. and Tang, X. 2007. Role of caspase-3 inhibitor in induced anoikis of mesenchymal stem cells *in vitro*. *J. Huazhong Univ. Sci. Technolog. Med. Sci.* **27**: 183–185.
7. Friis, N. F. and Feenstra, A. A. 1994. Mycoplasma hyorhinis in the etiology of serositis among piglets. *Acta Vet. Scand.* **35**: 93–98.
8. Frisch, S. M. and Francis, H. 1994. Disruption of epithelial cell-matrix interactions induces apoptosis. *J. Cell Biol.* **124**: 619–626.
9. Fujisawa, H., Ogura, T., Kurashima, Y., Yokoyama, T., Yamashita, J. and Esumi, H. 1994. Expression of two types of nitric oxide synthase mRNA in human neuroblastoma cell lines. *J. Neurochem.* **63**: 140–145.
10. Green, L. C., Wagner, D. A., Glogowski, J., Skipper, P. L., Wishnok, J. S. and Tannenbaum, S. R. 1982. Analysis of nitrate, nitrite, and [15N] nitrate in biological fluids. *Anal. Biochem.* **126**: 131–138.
11. Harasawa, R., Mizusawa, H., Nozawa, K., Nakagawa, T., Asada, K. and Kato, I. 1993. Detection and tentative identification of dominant mycoplasma species in cell cultures by restriction analysis of the 16S–23S rRNA intergenic spacer regions. *Res. Microbiol.* **144**: 489–493.
12. Jansson, E., Backman, A., Hakkarainen, K., Miettinen, A. and Seniusova, B. 1983. Mycoplasmas and arthritis. *Z Rheumatol.* **42**: 315–319.
13. Kagemann, G., Henrich, B., Kuhn, M., Kleinert, H. and Schnorr, O. 2005. Impact of Mycoplasma hyorhinis infection on L-arginine metabolism: differential regulation of the human and murine iNOS gene. *Biol. Chem.* **386**: 1055–1063.
14. Ketcham, C. M., Anai, S., Reutzel, R., Sheng, S., Schuster, S. M. and Brenes, R. B., Agbandje-McKenna, M., McKenna, R., Rosser, C. J. and Boehlein, S. K. 2005. p37 Induces tumor invasiveness. *Mol. Cancer Ther.* **4**: 1031–1038.
15. Kobayashi, H., Morozumi, T., Munthali, G., Mitani, K., Ito, N. and Yamamoto, K. 1996. Macrolide susceptibilityof *Mycoplasma hyorhinis* isolated from piglets. *Antimicrob. Agents Chemother.* **40**: 1030–1032.
16. Lipton, S. A., Choi, Y. B., Pan, Z. H., Lei, S. Z., Chen, H. S., Sucher, N. J., Loscalzo, J., Singel, D. J. and Stamler, J. S. 1993. A redox-based mechanism for the neuroprotective and neurodestructive effects of nitric oxide and related nitroso-compounds. *Nature* **364**: 626–632.
17. Mayer, B. and Hemmens, B. 1997. Biosynthesis and action of nitric oxide in mammalian cells. *Trends Biochem. Sci.* **22**: 477–481.
18. Mignotte, B. and Vayssiere, J. L. 1998. Mitochondria and apoptosis. *Eur. J. Biochem.* **252**: 1–15.
19. Morita, T., Fukuda, H., Awakura, T., Shimada, A., Umemura, T., Kazama, S. and Yagihashi, T. 1995. Demonstration of *Mycoplasma hyorhinis* as a possible primary pathogen for porcine otitis media. *Vet. Pathol.* **32**: 107–111.

20. Nakai, K., Urushihara, M., Kubota, Y. and Kosaka, H. 2003. Ascorbate enhances iNOS activity by increasing tetrahydrobiopterin in RAW 264.7 cells. *Free Radic. Biol. Med.* 35: 929–937.
21. Obara, H. and Harasawa, R. 2007. L-ascorbic acid enhances apoptosis in human gastric carcinoma cell line AZ-521 cells infected with *Mycoplasma hyorhinis*. *J. Vet. Med. Sci.* 70: 11–15.
22. Ouse, J. A. and House, C. A. 1992. Bacterial diseases. pp. 543–544. *In*: Disease of Swine 7th ed. (Taylor, D. J. ed.), Wolfe Publishing Ltd., England.
23. Paddenberg, R., Weber, A., Wulf, S. and Mannherz, H. G. 1989. Mycoplasma nucleases able to induce internucleosomal DNA degradation in cultured cells possess many characteristics of eukaryotic apoptotic nucleases. *Cell Death Differ.* 5: 517–528.
24. Rasper, D. M., Vaillancourt, J. P., Hadano, S., Houtzager, V. M., Seiden, I., Keen, S. L., Tawa, P., Xanthoudakis, S., Nasir, J., Martindale, D., Koop, B. F., Peterson, E. P., Thornberry, N. A., Huang, J., MacPherson, D. P., Black, S. C., Hornung, F., Lenardo, M. J., Hayden, M. R., Roy, S. and Nicholson, D. W. 1998. Cell death attenuation by 'Usurpin', a mammalian DED-caspase homologue that precludes caspase-8 recruitment and activation by the CD-95 (Fas, APO-1) receptor complex. *Cell Death Differ.* 5: 271–288.
25. Razin, S. 1992. Mycoplasma taxonomy and ecology. pp. 3–22. *In*: Mycoplasmas: Molecular Biology and Pathogenesis (Maniloff, j., McElhaney, R. N., Finch, L. R. and Baseman, J. B. eds.), American Society for Microbiology, Washington, D.C.
26. Sasaki, H., Igaki, H., Ishizuka, T., Kogoma, Y., Sugimura, T. and Terada, M. 1995. Presence of *Streptococcus* DNA sequence in surgical specimens of gastric cancer. *Jpn. J. Cancer Res.* 86: 791–794.
27. Slee, E. A., Harte, M. T., Kluck, R. M., Wolf, B. B., Casiano, C. A., Newmeyer, D. D., Wang, H. G., Reed, J. C., Nicholson, D. W., Alnemri, E. S., Green, D. R. and Martin, S. J. 1999. Ordering the cytochrome c-initiated caspase cascade: hierarchical activation of caspases-2, -3, -6, -7, -8, and -10 in a caspase-9-dependent manner. *J. Cell Biol.* 144: 281–292.
28. Takeichi, M., Inuzuka, H., Shimamura, K., Matsunaga, M. and Nose, A. 1990. Cadherin-mediated cell-cell adhesion and neurogenesis. *Neurosci. Res. (Suppl.)* 13: S92–S96.
29. Vicente, S., Perez-Rodriguez, R., Olivan, A. M., Martinez, Palacian, A., Gonzalez, M. P. and Oset-Gasque, M. J. 2006. Nitric oxide and peroxynitrite induce cellular death in bovine chromaffin cells: evidence for a mixed necrotic and apoptotic mechanism with caspases activation. *J. Neurosci. Res.* 84: 78–96.
30. Wyllie, A. H. 1992. Apoptosis and the regulation of cell numbers in normal and neoplastic tissues: an overview. *Cancer Metastasis Rev.* 11: 95–103.
31. Yamane, D., Nagai, M., Ogawa, Y., Tohya, Y. and Akashi, H. 2005. Enhancement of apoptosis via an extrinsic factor, TNF-alpha, in cells infected with cytopathic bovine viral diarrhea virus. *Microbes. Infect.* 7: 1482–1491.

NOTE *Bacteriology*

Novel Hemoplasma Species Detected in Free-Ranging Sika Deer (*Cervus nippon*)

Yusaku WATANABE[1,2,3], Masatoshi FUJIHARA[1,2], Hisato OBARA[1,2], Kazuei MATSUBARA[4], Kiyoshi YAMAUCHI[5] and Ryô HARASAWA[1,2]*

[1]*Department of Veterinary Microbiology, Faculty of Agriculture, Iwate University, Morioka 020–8550,* [2]*Department of Applied Veterinary Science, The United Graduate School of Veterinary Sciences, Gifu University, Gifu 501–1193,* [3]*Bremen Vet Center, Yahaba 028–3602,* [4]*Department of Animal Sciences, Faculty of Agriculture, Iwate University, Morioka 020–8550 and* [5]*Research Institute for Environmental Sciences and Public Health of Iwate Prefecture, Morioka 020–8570, Japan*

(Received 30 May 2010/Accepted 29 June 2010/Published online in J-STAGE 13 July 2010)

ABSTRACT. Hemoplasma infections in wild ungulates have not been reported yet in Japan. We examined presence of hemoplasmas in blood samples collected from 147 sika deer (*Cervus nippon*) in the Iwate prefecture by real-time PCR, and found 13 (9%) were positive. Almost entire region of the 16S rRNA gene of the representative strains from positive samples was amplified by conventional PCR. The nucleotide sequences of the 16S rRNA gene were further determined and compared with those of other hemoplasmas. Our examinations 1st revealed the presence of 2 distinct hemoplasma species in sika deer, which are previously not described. One of them was closely related to *M. ovis* by the 16S rRNA sequence analysis, but was found distinct by comparison of the RNase P RNA gene sequences. Pathogenicity of these two hemoplasma species in sika deer is currently unknown.

KEY WORDS: hemoplasma, mycoplasma, sika deer.

J. Vet. Med. Sci. 72(11): 1527–1530, 2010

Hemoplasmas are tiny epierythrocytic bacterial parasites that lack a cell wall like other mycoplasmas, but have never been cultured *in vitro* [6]. Hemoplasmas infections, may lead to hemolytic anemia in animals, have been reported in wild ungulates such as reindeer (*Rangifer tarandus*) raised on a farm in Michigan [12] and splenectomized deer captured from a wild population in Texas [5] in the United States. However prevalence of hemoplasma infections in free-living ungulates have not well been understood. Sika deer (*Cervus nippon*), middle-sized ungulates, are found in the temperate forests of eastern Asia, and Japan has large populations of native sika deer. Therefore, we have examined hemoplasma infections among free-ranging sika deer in Japan.

Blood samples were collected from 147 wild sika deer hunted for the population control measures in Iwate prefecture, Japan from 2004 to 2006, and stored at –20°C prior to examination. Total DNA was extracted from 200 μl blood samples collected from sika deer using the QIAamp DNA Blood Mini Kit (Qiagen, Hilden, Germany) according to the manufacturer's instructions. Negative controls consisting of 200 μl phosphate-buffered saline were prepared with each batch. Extracted DNA samples were stored at –80 °C prior to use.

For the preliminary screening of hemoplasma infections, specific PCR primers (forward primer: 5'-ATATTCCTACGGGAAGCAGC-3' and reverse primer: 5'-ACCGCAGCTGCTGGCACATA-3') for the 16S rRNA gene of hemoplasmas were used as described previously [9]. Real-time PCR was performed in a SmartCycler instrument (Cepheid, Sunnyvale, CA) with SYBR Premix Ex *Taq* (Code #RR041A, TaKaRa Bio., Shiga). The reaction mixture contained 1 μl of each primer (10 pmol/μl), 12.5 μl of 2X premix reaction buffer and water to volume of 23 μl. Finally, 2 μl of DNA samples as templates were added to this mixture. Amplification was achieved with 40 cycles of denaturation at 95°C for 5 sec, renaturation at 57°C for 20 sec, and elongation at 72°C for 15 sec, after the initial denaturation at 94°C for 30 sec. Fluorescence readings in a channel for SYBR Green I were taken throughout the experiments.

After real-time PCR, melting experiment was performed from 60 to 95°C at 0.2°C/sec with smooth curve setting averaging one point. Melting peaks were visualized by plotting the first derivative against the melting temperature (*Tm*) as described previously [2]. The *Tm* was defined as a peak of the curve, and if the highest point was a plateau, then the mid-point was identified as the *Tm*. The input amount of DNA, the copy number of the target as well as presence of co-infections with several targets did not influence the *Tm*. Out of the 147 blood samples tested by real-time PCR, 13 (9%) were found to be positive for hemplasma infection. The *Tm* of the positive samples was 82.79 ± 0.18°C.

The positive samples were further subjected to conventional PCR to amplify entire region of the 16S rRNA gene. The conventional PCR was carried out with 50-μl reaction mixtures containing 1 μl of DNA solution, 0.5 m*l* of TaKaRa LA *Taq* ™ (5 units/μl), 5 μl of 10X LA PCR™ Buffer II, 8 μl of 25 mM $MgCl_2$ (final 4.0 mM), 8 μl of dNTP mixture (2.5 mM each), 0.2 μl of forward primer (5'-AGAGTTTGATCCTGGCTCAG-3', equivalent to nucleotide numbers 11 to 30 of *M. wenyonii* (AY946266), or 5'-ATATTCCTACGGGAAGCAGC-3', equivalent to nucleotide numbers 328 to 347 of *M. wenyonii*), reverse primer (5'-ACCGCAGCTGCTGGCACATA-3', equivalent to

* CORRESPONDENCE TO: Prof. HARASAWA, R., Department of Veterinary Microbiology, Faculty of Agriculture, Iwate University, Morioka 020–8550, Japan.
e-mail: harasawa-tky@umin.ac.jp

nucleotide numbers 503 to 522 of *M. wenyonii*, or 5'-TAC-CTTGTTACGACTTAACT-3', equivalent to nucleotide numbers 1446 to 1465 of *M. wenyonii*) (50 pmol/μl each) and water to a final volume of 50 μl. After the mixture was overlaid with 20 μl of mineral oil, the reaction cycle was carried out 35 times with denaturation at 94°C for 30 sec, annealing at 58°C for 120 sec and extension at 72°C for 60 sec in a thermal cycler. Conventional PCR products that showed a clearly visible band were subjected to direct sequencing and the nucleotide sequences of the almost entire region of the 16S rRNA gene have been deposited to the DNA database under the accession numbers AB558897 to AB558899. The remaining 10 samples are still examined for determination of the nucleotide sequences.

The 16S rRNA gene sequences from the sika deer isolates were aligned with other hemoplasma sequences from DNA database using Clustal W [12]. An unrooted phylogenetic tree was generated with the neighbor-joining method [10] from a distance matrix corrected for nucleotide substitutions by the Kimura two-parameter model [4]. The dataset was resampled 1,000 times to generate bootstrap values (Fig. 1). 16S rRNA gene sequences of the two strains, Sika99 and Sika122, from the blood samples of sika deer showed 100% homology each other, but were distinct from the sequence of Sika152. The 16S rRNA gene sequences are widely used in microbiology for assigning uncultivable microorganisms as new species, and reclassification of haemotropic *Mycoplasma* species has been based on the16S rRNA gene sequences [7, 8]. In our examinations, hemoplasmas were divided into two genetic groups, haemofelis and wenyonii clusters, and the hemoplasmas detected in sika deer were both assigned into the wenyonii cluster.

This is the 1st demonstration of the existence of 2 genetically distinct hemoplasma species in sika deer. Although Sika99 and Sika122 showed close relatedness to '*Candidatus* M. haemotaradirangiferis' detected from reindeer [12], similarity of the 16S rRNA gene sequences between them was 95.7%, suggesting different species [1]. Thus, we ten-

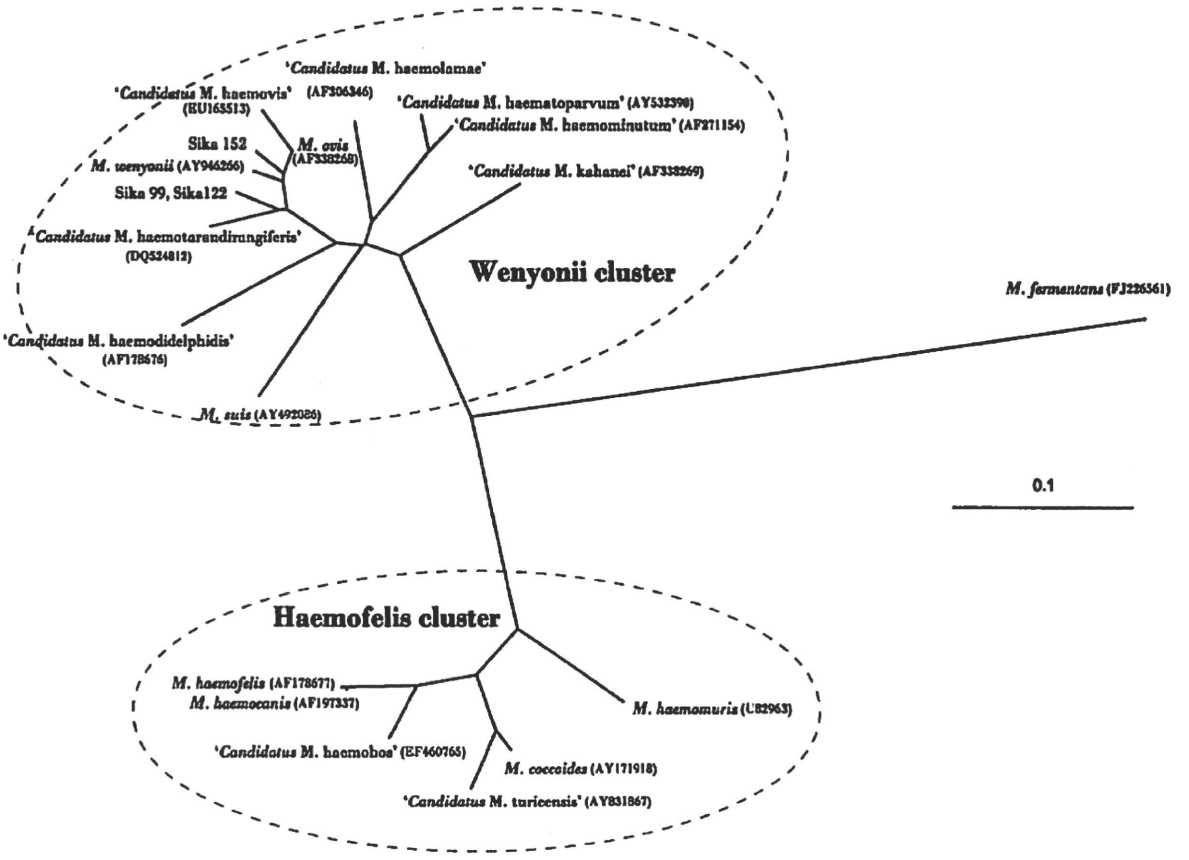

Fig. 1. An unrooted phylogenetic tree based on the 16S rRNA gene sequence comparison among mycoplasmas including 16 hemoplasma species (accession numbers are given in a parenthesis) and putative taxa created by Sika99, Sika122 and Sika152. Genetic distances were computed with CLUSTAL W [14]. Hemoplasmas were divided into two genetic clusters, haemofelis and wenyonii. A nucleotide sequence of the 16S rRNA gene of *M. fermentans* PG18 strain with accession number FJ226561 was included as an out-group. Sika99, Sika122 and Sika152 represent hemoplasma strains detected from the sika deer in the Iwate prefecture. Numbers in the relevant branches refer to the values of boot-strap probability of 1,000 replications. Scale bar indicates the estimated evolutionary distance.

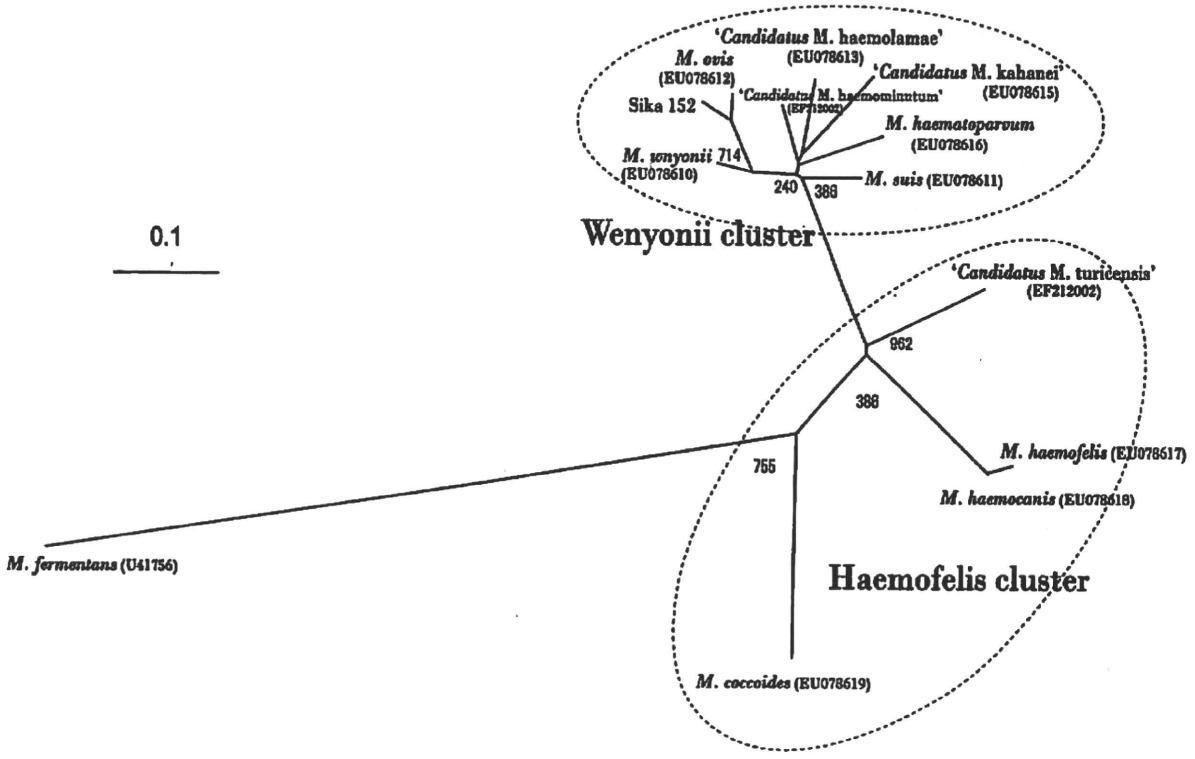

Fig. 2. An unrooted phylogenetic tree generated by comparison of the RNase P RNA (*rnpB*) gene sequences among mycoplasmas including 11 established species (accession numbers are given in a parenthesis) and a putative taxon created by Sika152. Genetic distances were computed with CLUSTAL W [14]. Two genetic clusters, haemofelis and wenyonii, were also revealed in this tree. A nucleotide sequence of the *rnpB* gene of *M. fermentans* with accession number U41756 was included as an out-group.Sika152 represents a hemoplasma sequence detected from the sika deer in the Iwate prefecture. Numbers in the relevant branches refer to the values of bootstrap probability of 1,000 replications. Scale bar indicates the estimated evolutionary distance.

tatively designated '*Candidatus* M. erythrocervae' for Sika99 and Sika122. On the other hand, Sika152 showed close relatedness to *M. ovis*, and sequence similarity between them was 98.4%, which may not be enough for establishment of a new species according to the cutoff value of the 16S rRNA gene sequence identity for species definition [1]. *M. ovis* is also close to '*Candidatus* M. haemovis', and their similarity is 97.9% [3]. Thus, we further examined the nucleotide sequence of the RNase P RNA (*rnpB*) gene of Sika152 to compare with other hemoplasma species [10]. The *rnpB* gene has been shown to be suitable for phylogenetic discrimination of closely related taxonomic groups when examined by 16S rRNA sequence comparison [13]. Partial nucleotide sequence of the *rnpB* gene of Sika152 was amplified by conventional PCR with forward primer rnpB-F (5'-AGTCTGAGATGACTRTAGTG-3' equivalent to nucleotide numbers 1 to 20 of *M. wenyonii* (EU078610)) and reverse primer rnpB-R (5'-TRCTTGMGGGGTTTGCCTCG-3' equivalent to nucleotide numbers 170 to 189 of *M. wenyonii* (EU078610)). Reaction was the same as used for the amplification of the 16S rRNA gene except for the annealing temperature at 60°C instead of 58°C. Amplified PCR product was subjected to direct sequencing and the nucleotide sequence of the *rnpB* gene of Sika152 has been deposited to the DNA database under the accession number AB561882. The *rnpB* gene sequence of Sika152 was aligned with other hemoplasma sequences from DNA databases using Clustal W [14]. A phylogenetic tree was constructed with the neighbor-joining method [11] from a distance matrix corrected for nucleotide substitutions by the Kimura two-parameter model [4]. The dataset was resampled 1,000 times to generate bootstrap values (Fig. 2). The *rnpB* gene sequence of Sika152 showed close relationship to *M. ovis* (90% similarity) as well as *M. wenyonii* (84%similarity), which was compatible with the results from the 16S rRNA gene comparison, and supported the notion that the Sika152 was distinct from other hemoplasma species. Similarly, *M. haemocanis* and *M. haemofelis* have been recognized as a distinct species due to difference of the *rnpB* gene, though they showed 99.2% homology in the 16S rRNA gene sequences. Therefore, we provisionally designated '*Candidatus* M. haemocervae' for Sika152.